THESIS FOR THE DEGREE OF
DOCTOR OF PHILOSOPHY

MOMENTUM-SPACE DYNAMICS OF RUNAWAY ELECTRONS IN PLASMAS

Adam Stahl

CHALMERS
UNIVERSITY OF TECHNOLOGY

Department of Physics
Chalmers University of Technology
Gothenburg, Sweden, 2017

MOMENTUM-SPACE DYNAMICS OF RUNAWAY ELECTRONS IN PLASMAS
Adam Stahl

ISBN 978-91-7597-532-0
Doktorsavhandlingar vid Chalmers tekniska högskola
Ny serie nr 4213
ISSN 0346-718X
Subatomic and Plasma Physics
Department of Physics
Chalmers University of Technology
SE-412 96 Gothenburg
Sweden
Telephone +46-(0)31-772 10 00

Printed by
Reproservice
Chalmers tekniska högskola
Gothenburg, Sweden, 2017

MOMENTUM-SPACE DYNAMICS OF RUNAWAY ELECTRONS IN PLASMAS

Adam Stahl
Department of Physics
Chalmers University of Technology

Abstract

Fast electrons in a plasma experience a friction force that decreases with increasing particle speed, and may therefore be continuously accelerated by sufficiently strong electric fields. These so-called runaway electrons may quickly reach relativistic speeds. This is problematic in tokamaks – devices aimed at producing sustainable energy through the use of thermonuclear fusion reactions – where runaway-electron beams carrying strong currents may form. If the runaway electrons deposit their kinetic energy in the plasma-facing components, these may be seriously damaged, leading to long and costly device shutdowns.

Crucial to the runaway phenomenon is the behavior of the runaway electrons in two-dimensional momentum space. The interplay between electric-field acceleration, collisional momentum-space transport, and radiation reaction determines the dynamics and the growth or decay of the runaway-electron population. In this thesis, several aspects of this interplay are investigated, including avalanche multiplication rates, synchrotron radiation reaction, modifications to the critical electric field for runaway generation, rapidly changing plasma parameters, and electron slide-away. Two numerical tools for studying electron momentum-space dynamics, based on an efficient solution of the kinetic equation, are presented and used throughout the thesis. The spectrum of the synchrotron radiation emitted by the runaway electrons – a useful diagnostic for their properties – is also studied.

It is found that taking the electron distribution into account properly is crucial for the interpretation of synchrotron spectra; that a commonly used numerical avalanche operator may either overestimate or underestimate the runaway-electron growth rate, depending on the scenario; that radiation reaction modifies the critical electric field, but that this modification often is small compared to other effects; that electron slide-away can occur at significantly weaker electric fields than expected; and that collisional nonlinearities may be significant for the evolution of runaway-electron populations in disruption scenarios.

Keywords: fusion-plasma physics, tokamak, runaway electrons, synchrotron radiation, critical electric field, slide-away, non-linear collision operator

Publications

This thesis is based on the work contained in the following papers:

A A. Stahl, M. Landreman, G. Papp, E. Hollmann, and T. Fülöp,
Synchrotron radiation from a runaway electron distribution in tokamaks,
Physics of Plasmas **20**, 093302 (2013).
http://dx.doi.org/10.1063/1.4821823
http://arxiv.org/abs/1308.2099

B M. Landreman, A. Stahl, and T. Fülöp,
Numerical calculation of the runaway electron distribution function and associated synchrotron emission,
Computer Physics Communications **185**, 847-855 (2014).
http://dx.doi.org/10.1016/j.cpc.2013.12.004
http://arxiv.org/abs/1305.3518

C A. Stahl, O. Embréus, G. Papp, M. Landreman, and T. Fülöp,
Kinetic modelling of runaway electrons in dynamic scenarios,
Nuclear Fusion **56**, 112009 (2016).
http://dx.doi.org/10.1088/0029-5515/56/11/112009
http://arxiv.org/abs/1601.00898

D A. Stahl, E. Hirvijoki, J. Decker, O. Embréus, and T. Fülöp,
Effective critical electric field for runaway electron generation,
Physical Review Letters **114**, 115002 (2015).
http://dx.doi.org/10.1103/PhysRevLett.114.115002
http://arxiv.org/abs/1412.4608

E A. Stahl, M. Landreman, O. Embréus, and T. Fülöp,
NORSE: A solver for the relativistic non-linear Fokker-Planck equation for electrons in a homogeneous plasma,
Computer Physics Communications **212**, 269-279 (2017).
http://dx.doi.org/10.1016/j.cpc.2016.10.024
http://arxiv.org/abs/1608.02742

F A. Stahl, O. Embréus, M. Landreman, G. Papp, and T. Fülöp,
Runaway-electron formation and electron slide-away in an ITER post-disruption scenario.
Journal of Physics: Conference Series **775**, 012013 (2016).
http://dx.doi.org/10.1088/1742-6596/775/1/012013
http://arxiv.org/abs/1610.03249

Statement of contribution

In Papers A, C, E and F, I performed all simulations and associated analysis, and produced all the figures. I wrote all the text in Papers C, E and F, and a majority of that in Paper A. In addition I did all of the programming associated with the code SYRUP used in Paper A and the tool NORSE described in Paper E, as well as most of the programming related to the capabilities of CODE described in Paper C. I performed the majority of the analytical calculations required for Papers A, C and E. In Paper B, I was mainly responsible for the work presented in Section 6, but in addition contributed to the remainder of the text. To a lesser extent, I was also involved in the development of the tool CODE described in the paper. In Paper D, I performed the numerical simulations, together with the associated implementation and analysis, produced the majority of the figures and text, and did some of the analytical calculations.

Additional publications, not included in the thesis

G O. Embréus, A. Stahl, and T. Fülöp,
Effect of bremsstrahlung radiation emission on fast electrons in plasmas,
New Journal of Physics **18**, 093023 (2016).
http://dx.doi.org/10.1088/1367-2630/18/9/093023
http://arxiv.org/abs/1604.03331

H J. Decker, E. Hirvijoki, O. Embréus, Y. Peysson, A. Stahl, I. Pusztai, and T. Fülöp,
Numerical characterization of bump formation in the runaway electron tail,
Plasma Physics and Controlled Fusion **58**, 025016 (2016).
http://dx.doi.org/10.1088/0741-3335/58/2/025016
http://arxiv.org/abs/1503.03881

I E. Hirvijoki, I. Pusztai, J. Decker, O. Embréus, A. Stahl, and T. Fülöp,
Radiation reaction induced non-monotonic features in runaway electron distributions,
Journal of Plasma Physics **81**, 475810502 (2015).
http://dx.doi.org/10.1017/S0022377815000513
http://arxiv.org/abs/1502.03333

J O. Embréus, S. Newton, A. Stahl, E. Hirvijoki, and T. Fülöp,
Numerical calculation of ion runaway distributions,
Physics of Plasmas **22**, 052122 (2015).
http://scitation.aip.org/content/aip/journal/pop/22/5/10.1063/1.4921661
http://arxiv.org/abs/1502.06739

K G. I. Pokol, A. Kómár, A. Budai, A. Stahl, and T. Fülöp,
Quasi-linear analysis of the extraordinary electron wave destabilized by runaway electrons,
Physics of Plasmas **21,** 102503 (2014).
http://dx.doi.org/10.1063/1.4895513
http://arxiv.org/abs/1407.5788

Conference contributions

L A. Tinguely, R. Granetz, and A. Stahl, *Analysis of Runaway Electron Synchrotron Emission in Alcator C-Mod*, Proceedings of the 58th Annual Meeting of the APS Division of Plasma Physics **61**, 18, TO4.00007 (2016). http://meetings.aps.org/Meeting/DPP16/Session/TO4.7

M C. Paz-Soldan, N. Eidietis, D. Pace, C. Cooper, D. Shiraki, N. Commaux, E. Hollmann, R. Moyer, R. Granetz, O. Embréus, T. Fülöp, A. Stahl, G. Wilkie, P. Aleynikov, D. P. Brennan, and C. Liu, *Synchrotron and collisional damping effects on runaway electron distributions*, Proceedings of the 58th Annual Meeting of the APS Division of Plasma Physics **61**, 18, CO4.00010 (2016). http://meetings.aps.org/Meeting/DPP16/Session/CO4.10

N O. Ficker, J. Mlynar, M. Vlainic, V. Weinzettl, J. Urban, J. Cavalier, J. Havlicek, R. Panek, M. Hron, J. Cerovsky, P. Vondracek, R. Paprok, J. Decker, Y. Peysson, O. Bogar, A. Stahl, and the COMPASS Team, *Long slide-away discharges in the COMPASS tokamak*, Proceedings of the 58th Annual Meeting of the APS Division of Plasma Physics **61**, 18, GP10.00101 (2016). http://meetings.aps.org/Meeting/DPP16/Session/GP10.101

O Y. Peysson, G. Anastassiou, J.-F. Artaud, A. Budai, J. Decker, O. Embréus, O. Ficker, T. Fülöp, K. Hizanidis, Y. Kominis, T. Kurki-Suonio, P. Lauber, R. Lohner, J. Mlynar, E. Nardon, S. Newton, E. Nilsson, G. Papp, R. Paprok, G. Pokol, F. Saint-Laurent, C. Reux, K. Sarkimaki, C. Sommariva, A. Stahl, M. Vlainic, and P. Zestanakis, *A European Effort for Kinetic Modelling of Runaway Electron Dynamics*, Theory and Simulation of Disruptions Workshop (2016). http://tsdw.pppl.gov/Talks/2016/Peysson.pdf

P T. Fülöp, O. Embréus, A. Stahl, S. Newton, I. Pusztai, and G. Wilkie, *Kinetic modelling of runaways in fusion plasmas*, Proceedings of the 26th IAEA Fusion Energy Conference, Kyoto, Japan, TH/P4–1 (2016).

Q O. Embréus, A. Stahl, and T. Fülöp, *Effect of bremsstrahlung radiation emission on fast electrons in plasmas*, Europhysics Conference Abstracts **40A**, O2.402 (2016). http://ocs.ciemat.es/EPS2016PAP/pdf/O2.402.pdf

R A. Stahl, O. Embréus, E. Hirvijoki, I. Pusztai, J. Decker, S. Newton, and T. Fülöp, *Reaction of runaway electron distributions to radiative processes*, Proceedings of the 57th Annual Meeting of the APS Division of Plasma Physics **60**, 19, PP12.00103 (2015). http://meetings.aps.org/link/BAPS.2015.DPP.PP12.103

S O. Embréus, A. Stahl, and T. Fülöp, *Conservative large-angle collision operator for runaway avalanches*, Proceedings of the 57th Annual Meeting of the APS Division of Plasma Physics **60**, 19, PP12.00107 (2015). http://meetings.aps.org/link/BAPS.2015.DPP.PP12.107

T S. Newton, O. Embréus, A. Stahl, E. Hirvijoki, and T. Fülöp, *Numerical calculation of ion runaway distributions,* Proceedings of the 57th Annual Meeting of the APS Division of Plasma Physics **60**, 19, CP12.00118 (2015). http://meetings.aps.org/link/BAPS.2015.DPP.CP12.118

U I. Pusztai, E. Hirvijoki, J. Decker, O. Embréus, A. Stahl, and T. Fülöp, *Non-monotonic features in the runaway electron tail*, Europhysics Conference Abstracts **39E**, O3.J105 (2015). http://ocs.ciemat.es/EPS2015PAP/pdf/O3.J105.pdf

V G. Papp, A. Stahl, M. Drevlak, T. Fülöp, P. Lauber, and G. Pokol, *Towards self-consistent runaway electron modelling*, Europhysics Conference Abstracts **39E**, P1.173 (2015). http://ocs.ciemat.es/EPS2015PAP/pdf/P1.173.pdf

W O. Embréus, S. Newton, A. Stahl, E. Hirvijoki, and T. Fülöp, *Numerical calculation of ion runaway distributions*, Europhysics Conference Abstracts **39E**, P1.401 (2015). http://ocs.ciemat.es/EPS2015PAP/pdf/P1.401.pdf

X A. Stahl, E. Hirvijoki, M. Landreman, J. Decker, G. Papp, and T. Fülöp, *Effective critical electric field for runaway electron generation*, Europhysics Conference Abstracts **38F**, P2.049 (2014). http://ocs.ciemat.es/EPS2014PAP/pdf/P2.049.pdf

Y G. Pokol, A. Budai, J. Decker, Y. Peysson, E. Nilsson, A. Stahl, A. Kómár, and T. Fülöp, *Interaction of oblique propagation extraordinary electron waves and runaway electrons in tokamaks*, Europhysics Conference Abstracts **38F**, P2.042 (2014). http://ocs.ciemat.es/EPS2014PAP/pdf/P2.042.pdf

Z A. Stahl, M. Landreman, T. Fülöp, G. Papp, and E. Hollmann, Synchrotron radiation from runaway electron distributions in tokamaks, Europhysics Conference Abstracts **37D**, P5.117 (2013). http://ocs.ciemat.es/EPS2013PAP/pdf/P5.117.pdf

Contents

Acknowledgments

The life of a doctoral student has sometimes been described as a stumbling journey down a seemingly endless dark tunnel. Not so in the Plasma Theory Group at Chalmers, where the guidance of Professor Tünde Fülöp provides a map, as well as the light by which to read it. I am fortunate and thankful to have had her support throughout my doctoral studies. In fact, I wish every doctoral student the privilege of having Tünde as their supervisor (although I recognize the logistical nightmare this would entail)!

I also owe a lot to my co-supervisors Dr. Matt Landreman and Dr. István Pusztai. Matt in particular has been involved on some level in most projects I have undertaken during these years and have identified (and often solved) many a problem I didn't even know I had. István has provided the stability (and ability) closer to home, always contributing knowledgeable input on all things plasma physics.

The plasma theory group would be nothing without its current and former members, of which there are many. Thanks for the marvelous physics and non-physics discussions, salty lunches, pizza parties and ski trips. I will miss you all. In particular I would like to thank my long-time roommate and close collaborator Ola Embréus for his remarkable insight and investigative journalism, and my short-time roommate and long-time friend Dr. Gergely Papp for his eagle eye and grounded feet.

Finally; the reason I leave the office in the evening with a smile on my face. Thank you Hedvig for providing distractions and focus, cookies and salads, insight and bogus, odd meters and ballads. Without these, no map in the world would see me through to the end of the tunnel.

Thank you all

1 Introduction

In plasma physics, many interesting phenomena occur that are outside of our everyday experience. One of these is the generation of so-called *runaway electrons* (or simply *runaways*) – electrons that under certain conditions are continuously accelerated by electric fields [1, 2]. The dynamics of the process is such that the runaways quickly reach relativistic energies; they move with speeds very close to that of light. The study of runaway electrons therefore combines two fascinating areas of physics: Einstein's special relativity [3], and plasma physics; giving rise to interesting dynamics (as well as complicated mathematics). As we shall see, runaways appear in a variety of atmospheric, astrophysical and laboratory contexts.

Apart from their intrinsic interest, these highly energetic particles are also a cause for concern in the context of fusion-energy experiments [4]. Generating electric power using controlled thermonuclear fusion reactions is a promising concept for a future sustainable energy source [5–7], but stable and controllable operating conditions are required for a successful fusion power plant. The presence of runaway electrons in the plasmas of fusion reactors under certain circumstances is one of the main remaining hurdles on the road to realization of fusion power production [8], as the runaways have the potential to severely damage the machine when they eventually leave the plasma and strike the wall [9]. In order to accurately assess the frequency of such events, as well as the resulting damage in a given situation, there is a great need to improve the understanding of the mechanisms that generate and suppress runaway electrons, and to better describe their dynamics [10].

In order for runaways to be generated, a comparatively long-lived electric field is needed. Due to the natural tendency of the plasma particles to rearrange in order to screen out such fields, they are not normally present in unmagnetized plasmas. However in certain situations, for instance if a current running through the plasma changes quickly or if the magnetic field lines in a magnetized plasma reconnect, an electric field is induced which may be sufficient to lead to runaway formation. Runaway electrons do form in atmospheric plasmas – they have been linked to for instance lightning discharges

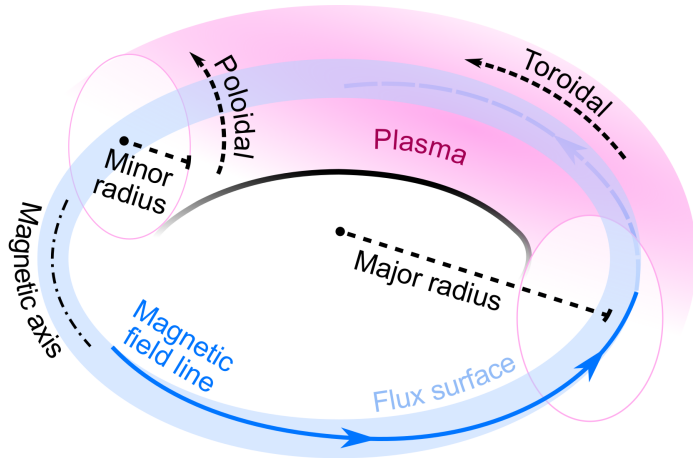

Figure 1.1: A tokamak plasma (pink), together with various common terms and concepts.

[11], impulsive radio emissions [12], and terrestrial gamma-ray flashes [13] – and in the mesosphere [14]. In astrophysical plasmas, they are expected to form in for instance solar flares [15] and large-scale filamentary structures in the galactic center [16]. Under certain circumstances, other plasma species may also run away. Both ion and positron runaway have been investigated in recent work (see Refs. [17–19], as well as Paper J, not included in the thesis). Our main interest in this thesis is however electron runaway in the context of magnetic-confinement thermonuclear fusion.

The most common type of fusion device is called a *tokamak* (see for instance [7, 20]). It uses strong magnetic fields to confine a plasma in which the fusion reactions between hydrogen-isotope ions take place. The charged particles in the plasma follow helical orbits (spirals) around the magnetic field lines due to the Lorentz force [21, 22], and are thus (to a first approximation) prevented from reaching the walls of the device. In a tokamak, the "magnetic cage" (and thus the plasma) has the form of a torus (a doughnut), as shown in Fig. 1.1. The torus shape can be thought of as being formed from a cylinder, bent around so that its two ends connect. The direction along the axis of this cylinder is referred to as *toroidal* (and the axis itself the *magnetic axis*), while

the direction around the circumference of the cylinder is called *poloidal* and its radius is the *minor radius*. The radius of the circle defined by the magnetic axis is called the *major radius*, and the relation between the major and minor radii is referred to as the *aspect ratio*. The plasma temperature and density are maximized close to the magnetic axis, and this is also where the runaways predominantly form. Due to the loop-like toroidal geometry, the magnetic field acts as an "infinite racetrack" for the runaways, which make millions of toroidal revolutions of the tokamak each second.

In order to achieve satisfactory plasma confinement, it is necessary to drive a strong current in the plasma. The poloidal magnetic field induced by the current introduces a helical twist to the magnetic field lines, and it can be shown that each field line covers a toroidal surface of constant pressure. The tokamak plasma can therefore be viewed as being made up of a series of such nested *flux surfaces*. The plasma current is generated using transformer action: a changing current is driven through a conducting loop interlocked with the tokamak vessel, and the change in this current induces a voltage (the so-called *loop voltage*) which drives a current in the plasma. Since a hot plasma is a very good conductor, the loop-voltage does not need to be particularly strong during normal operation (it is usually of order 1 V), and tokamak plasmas (*discharges* or "shots") are routinely maintained for several seconds, and sometimes for several minutes or more. Inductive current drive does not enable continuous (steady-state) operation, however, and the tokamak is fundamentally a pulsed device (in the absence of auxiliary current-drive systems).

During the start-up of a tokamak discharge, a plasma is formed by the ionization of a gas. For this process, a strong electric field is usually needed. Runaways may form in this situation [23–25], however their formation can usually be avoided by maintaining a high enough gas/plasma density. The case of a changing current is more problematic. Abrupt changes in plasma current occur during so-called *disruptions*, in which the plasma becomes unstable, rapidly cools down due to a loss of confinement, and eventually terminates [8, 26, 27]. As the plasma cools, the resistivity increases drastically (since it is proportional to $T^{-3/2}$), and a large electric field is induced which tries to maintain the current (in accordance with Lenz's law [28]). Near the magnetic axis, this field is often strong enough to lead to runaway generation, and runaway beams in the center of the plasma have been observed during disruptions in many tokamaks (for instance JET [29–31], DIII-D [32, 33], Alcator C-Mod [34], Tore Supra [35], KSTAR [36], COMPASS [37], ASDEX Upgrade [38] and TCV [39]). Runaways can also be generated in so-called sawtooth crashes [40], and even during normal stable operation if the density

is low enough [39, 41, 42] (the accelerating field in this case is the normal loop voltage). Some auxiliary plasma-heating schemes produce an elevated tail in the electron velocity distribution which can lead to increased runaway production, should a disruption occur [39, 43].

The runaways predominantly form close to the magnetic axis of the tokamak, where the flux-surface radius is small compared to the major radius. Many aspects of the fundamental runaway dynamics can therefore be studied in the large–aspect-ratio limit where transverse spatial effects can be neglected. Since the plasma is essentially homogeneous in the direction along the magnetic field, the spatial dependence can be neglected entirely, and for an understanding of the basic mechanisms it is sufficient to treat the runaway process purely in momentum-space. As discussed in Sec. 3.1, one of the momentum-space coordinates (the angle describing the gyration around the field lines), can be averaged over, reducing the problem to two momentum-space dimensions. These simplifications are done throughout this thesis, except for parts of Paper A (where a radial dependence is included). In practice, the situation is more complicated, however, and spatial effects are often important, as will be discussed in Sec. 2.3. Several numerical tools that take magnetic-trapping and radial diffusive-transport effects into account (such as `LUKE` [44–46] and `CQL3D` [47, 48]) also exist.

The main reason for the interest in runaway research is that the runaways pose a serious threat to tokamaks. During disruptions, a large fraction of the initial plasma current (which is often several megaamperes) can be converted into runaway current. The runaways are normally well-confined in the tokamak, but a variety of mechanisms (such as instabilities or a collective displacement of the entire runaway beam) can transport them out radially. Unless their generation is successfully mitigated, or runaway-beam stability can be externally enforced, the runaways eventually escape the plasma and strike the wall where they can destroy sensitive components or degrade the wall material [49].

In present-day tokamaks, runaways are a nuisance, but usually not a serious threat (although there are exceptions, see for instance Ref. [31]). However, the avalanche multiplication (see Sec. 2.2.3) of a primary runaway seed is predicted to scale exponentially with plasma current [50], and it is believed that in future devices which will have a larger current (such as the International Thermonuclear Experimental Reactor ITER [51, 52] and eventually commercial fusion reactors), the problem will be much more severe. In these devices, disruptions can essentially not be tolerated at all and much effort is devoted to research on runaway and disruption mitigation techniques [10, 33, 49, 53].

This thesis focuses on the dynamics of the runaway electrons in momentum space, their generation and loss, and the forces that affect them. Most of the results presented herein are not specific to fusion plasmas or a tokamak magnetic geometry, however we will make use of fusion-relevant plasma parameters throughout. The majority of the work described in this thesis was conducted using two numerical tools developed as part of the thesis work: `CODE`, described in Papers B and C; and `NORSE`, described in Paper E. With these tools, all three major runaway-generation mechanisms (Dreicer generation, hot-tail generation and avalanche generation through knock-on collisions – to be discussed in Sec. 2.2), as well as two important energy-loss mechanisms (synchrotron and bremsstrahlung radiation emission) can be studied in detail. Synchrotron radiation is particularly important, and will be discussed in Chapter 4. It is also the main subject of Papers A and D – as a diagnostic for the runaway distribution and as a damping mechanism for runaway growth, respectively.

Let us now turn to discussing the basic mechanisms responsible for the runaway phenomenon, and the quantities characterizing the runaway dynamics.

2 Runaway-electron generation and loss

In short, a runaway electron is an electron in a plasma which experiences a net accelerating force during a substantial time – enough to give it a momentum significantly larger than that of the electrons in the thermal population.

The accelerating force on the electron is supplied by an electric field $\mathbf{E}$, so that $\mathbf{F}_{\mathrm{E}} = -e\mathbf{E}$, where e is the elementary charge. Meanwhile, Coulomb interaction with the other particles in the plasma (commonly referred to as *collisions*) introduces a friction force $\mathbf{F}_{\mathrm{C}}(v)$. The origin of the runaway phenomenon is that $\mathbf{F}_{\mathrm{C},\parallel}$, the component of the friction force parallel to the electric (or magnetic, if the plasma is magnetized) field, is a nonmonotonic function of the particle velocity, with a maximum around the electron thermal speed (v_{th}) [54], as illustrated in Fig. 2.1. Therefore $\partial\mathbf{F}_{\mathrm{C},\parallel}/\partial v < 0$ for particles that are faster than v_{th} – the friction force on these particles *decreases* with increasing particle velocity. The physical origin of this effect is that the faster particles spend less time in the vicinity of other particles in the plasma; as the particle speed increases, the impulse delivered to the fast particle in each encounter decreases more rapidly than the number of encounters increases, leading to a reduction in the friction [54]. This implies that if the accelerating force is sufficient to overcome the friction at the current velocity v_0 of the particle, $|\mathbf{F}_{\mathrm{E}}| > \mathbf{F}_{\mathrm{C},\parallel}(v_0)$, it will be able to accelerate the particle for all $v > v_0$, i.e. the particle will be continuously accelerated to relativistic energies – it will *run away* – as long as the electric field persists.

2.1 The runaway region of momentum space

For an electric field of intermediate strength ($E_{\mathrm{c}} < E < E_{\mathrm{sa}}$, with the critical field E_{c} and slide-away field E_{sa} to be defined in this section), there exist some velocities for which the acceleration by the electric field overcomes the

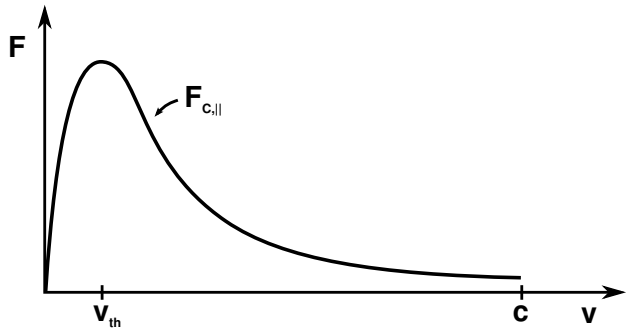

Figure 2.1: Friction force on an electron due to collisions, as a function of its velocity (schematic).

collisional friction. These velocities constitute the *runaway region* S_r in velocity space, indicated in Fig. 2.2. If only collisional friction is considered, this region is semi-infinite in momentum space, extending from some lowest *critical momentum* p_c to arbitrarily high momenta, due to the dependence of the friction force on velocity, as discussed above. The particles that are not in the runaway region are only to a lesser extent affected by the electric field, since the collisions dominate their dynamics.

Due to the directivity of the electric field, the force balance is not homogeneous in velocity. Several other forces also affect the dynamics, in particular radiation-reaction forces associated with synchrotron and bremsstrahlung emission. In these cases, the force balance is altered, ultimately preventing the electrons from reaching arbitrarily high momenta (this is the motivation for the use of the slightly vague definition of runaway at the beginning of this chapter). How to determine the runaway region in these more general situations is discussed in Sec. 2.1.3.

Furthermore, the picture is complicated by the fact that not only friction due to Coulomb collisions (collisional slowing down) contributes to the dynamics. The collisions also lead to diffusion of the electrons in velocity space: both parallel to the particle velocity and perpendicular to it (referred to as *pitch-angle scattering*). The diffusion is caused by velocity-space gradients in the distribution of particle velocities (see Sec. 3.1), parallel and perpendicular to v for the two effects, respectively. Pitch-angle scattering does not directly affect the energy of the electron, but is important for the behavior in two-dimensional velocity space (see for instance [54] for a comprehensive introduction to collisional phenomena). In general, the full evolution of the runaway population can only be obtained using numerical simulations.

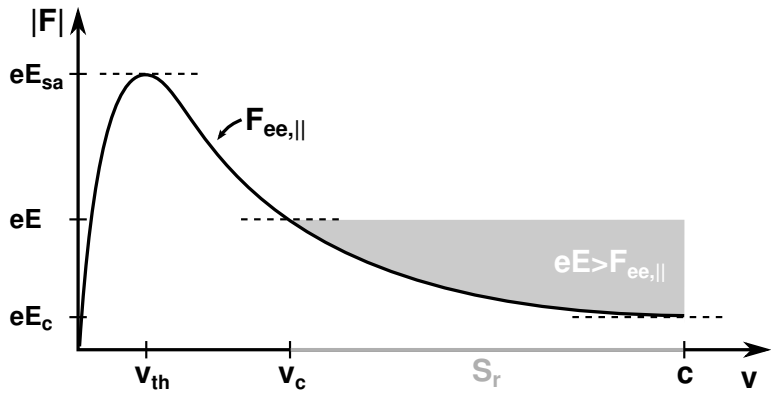

Figure 2.2: Forces corresponding to collisional friction against electrons ($F_{\mathrm{ee},\parallel}$), the critical field ($E_{\mathrm{c}}$) and the slide-away field (E_{sa}). The runaway region in velocity space (S_{r}) associated with the electric field E is shown as the gray part of the velocity axis.

2.1.1 Critical electric field and critical momentum

The *critical electric field* for runaway electron generation, E_{c}, is the weakest field at which runaway is possible, see Fig. 2.2. The accelerating force due to E_{c} is simply equal (and opposite) to the sum of all the forces acting to slow the particle down, at the speed v_{min} where they are minimized: $e\mathbf{E}_{\mathrm{c}} = \min\left(\sum_i \mathbf{F}_{\mathrm{f},i}(v)\right) = \sum_i \mathbf{F}_{\mathrm{f},i}(v_{\mathrm{min}})$. In the simplest case, the only retarding force is due to collisions with electrons (due to the mass difference, the energy lost by the electrons in collisions with ions is neglected, as are all other forces): $eE_{\mathrm{c}} = F_{\mathrm{ee},\parallel}(v = v_{\mathrm{min}})$. In this case, it is easy to obtain an expression for E_{c}. The friction force on a highly energetic electron is given by [54]:

$$F_{\mathrm{ee},\parallel}(v) = \frac{1}{v^2}\, m_{\mathrm{e}} c^3 \nu_{\mathrm{rel}}, \tag{2.1}$$

where v is the speed of the particle, c is the speed of light, m_{e} is the electron rest mass and

$$\nu_{\mathrm{rel}} = \frac{n_{\mathrm{e}} e^4 \ln\Lambda}{4\pi\varepsilon_0^2 m_{\mathrm{e}}^2 c^3} \tag{2.2}$$

is the *collision frequency* for a highly relativistic electron. Here n_{e} is the number density of electrons, $\ln\Lambda$ is the Coulomb logarithm (see for instance Refs.

[54, 55]) and ε_0 is the vacuum permittivity. The collision frequency is defined such that $1/\nu$ is (approximately) the average time for a particle to experience a 90° deflection due to an accumulation of small-angle Coulomb interactions (which are much more frequent than large-angle collisions in fusion plasmas).

The friction force in Eq. (2.1) is minimized as $v \to c$ (we have already mentioned that $F_{\mathrm{ee},\parallel}$ is monotonically decreasing for large velocities)[1]. We thus have that the critical field is $E_\mathrm{c} = F_{\mathrm{ee},\parallel}(v \to c)/e$, or

$$E_\mathrm{c} = \frac{m_\mathrm{e} c}{e}\nu_\mathrm{rel} = \frac{n_\mathrm{e} e^3 \ln\Lambda}{4\pi\varepsilon_0^2 m_\mathrm{e} c^2}, \tag{2.3}$$

which was obtained by Connor and Hastie in 1975 [56]. As discussed in Paper D and Sec. 4.2.2, synchrotron radiation reaction leads to an increase in the critical field as the minimum of the friction force is effectively raised. Since the synchrotron radiation-reaction force vanishes along the parallel axis, this is however an effect of dynamics in 2D momentum-space and cannot be easily accounted for in the simple model considered here.

For any $E > E_\mathrm{c}$, there exists some speed v_c above which the electric field overcomes the friction force. Particles with a velocity greater than this critical speed will run away, and v_c thus marks the lower boundary of the runaway region (in the parallel direction), as illustrated in Fig. 2.2. It is customary to study runaways in terms of momentum rather than velocity. The *critical momentum* is a simple function of the electric field strength if expressed in terms of the normalized momentum $p = \gamma v/c$, where $\gamma = 1/\sqrt{1 - v^2/c^2}$ is the relativistic mass factor:

$$p_\mathrm{c} = \frac{1}{\sqrt{E/E_\mathrm{c} - 1}}, \tag{2.4}$$

if the electron is assumed to move parallel to the electric field [56]. Similarly, the corresponding critical γ is $\gamma_\mathrm{c} = \sqrt{(E/E_\mathrm{c})/(E/E_\mathrm{c} - 1)}$.

2.1.2 Dreicer and slide-away fields

The critical field E_c corresponds to the field balancing the minimum of the collisional friction force. The *Dreicer field,* E_D [1, 2], on the other hand,

[1] Like much of plasma physics, this result assumes that the Coulomb logarithm $\ln\Lambda$ is a constant. In reality, it is energy dependent and increases logarithmically with p for large p. The minimum of the friction force is correspondingly found at v somewhat below c, however the value of E_c is only moderately affected.

approximately balances the maximum of the friction force, which is located around $v = v_{\mathrm{th}}$, with $v_{\mathrm{th}} = \sqrt{2T_{\mathrm{e}}/m_{\mathrm{e}}}$ the electron thermal speed and T_{e} the electron temperature[2]. The critical and Dreicer fields are related by the ratio of the thermal energy to the electron rest energy:

$$E_{\mathrm{D}} = \frac{m_{\mathrm{e}}c^2}{T_{\mathrm{e}}} E_{\mathrm{c}} = \frac{n_{\mathrm{e}} e^3 \ln\Lambda}{4\pi\varepsilon_0^2 T_{\mathrm{e}}}. \tag{2.5}$$

For fields stronger than the *slide-away field* $E_{\mathrm{sa}} \simeq 0.214 E_{\mathrm{D}}$ [1], the accelerating force overcomes the friction at all particle velocities, and the whole electron population thus runs away. This phenomenon is called *slide-away* [57].

In practice, the electric field in a fusion plasma is almost always much smaller than the Dreicer and slide-away fields. Therefore runaway dynamics can usually be studied in the regime where $E_{\mathrm{c}} < E \ll E_{\mathrm{sa}}$ is fulfilled, in which case the runaways can be treated as a small perturbation to a velocity distribution that is close to local thermal equilibrium (i.e. a Maxwellian). If the electric field is comparable to E_{sa}, however; the distribution will deviate strongly from a Maxwellian shape. This will in turn lead to a reduction in the friction in the bulk and a corresponding decrease in the slide-away field. Thus – as discussed in Sec. 5.2 – even though $E < E_{\mathrm{sa}}$ initially, a transition to slide-away can quickly occur due to the distortion of the distribution caused by the strong electric field.

2.1.3 General calculation of the runaway region

Let us now discuss how to define the runaway region in the full two-dimensional momentum space. The two momentum-space dimensions are conveniently parametrized by the coordinates (p, ξ), where $p = \gamma v/c$ is the normalized momentum and $\xi = p_{||}/p$ is the cosine of the particle pitch angle (which characterizes the pitch of the helix that describes the particle orbit around a magnetic field line). These coordinates are suitable for analytical as well as numerical calculations, and will therefore be used throughout much of the remainder of this thesis. In the definition of ξ, $p_{\parallel}$ is the component of the momentum parallel to the magnetic field and similarly $p_{\perp}$ is the perpendicular component. The coordinates $(p_{\parallel}, p_{\perp})$ are convenient for visualizing the distribution and will therefore be used in several figures throughout the thesis. Note also that the relativistic mass factor is related to p through $\gamma^2 = p^2 + 1$.

[2]It is customary in plasma physics to let $T_{\mathrm{e}} \equiv k_{\mathrm{B}} T_{\mathrm{e}}$, so that the "temperature" actually is the thermal energy, and to express it in eV.

In general, the object of interest when studying runaway-electron dynamics is the distribution function f of electron momenta, which will be thoroughly introduced in Sec. 3.1. For the following discussion, we just note that the runaways normally form a narrow tail in the distribution function, centered around the parallel axis (i.e. at $\xi \approx 1$), whereas the contours of the equilibrium (*Maxwellian*) distribution form concentric half circles in the $(p_\parallel, p_\perp)$-plane, as illustrated in Fig. 2.3.

The lower boundary of the runaway region in 2D momentum-space is often called the *separatrix*, as it separate two regions with distinct dynamical properties. It is well-defined in the parallel direction where it takes the value $p = p_\mathrm{c}$ [56], however there are several ways to express its dependence on the pitch angle. In the following discussion, an unambiguous separatrix in momentum space is obtained by neglecting the effect of collisional diffusion.

A common definition of the separatrix divides momentum space into two regions based on whether the accelerating electric field or the friction from Coulomb collisions dominate. The boundary between these regions is described by $p = p_\mathrm{s}$, with

$$p_\mathrm{s}^2(\xi) = (\xi E/E_\mathrm{c} - 1)^{-1} \tag{2.6}$$

(see for instance Paper H). At the parallel axis ($\xi = 1$), we find $p_\mathrm{s}(1) = p_\mathrm{c}$, as expected.

Equation (2.6) does not take into account the fact that in 2D, the electric field can accelerate a particle into the runaway region, even though it experiences a net slowing-down force (i.e. is not in the runaway region initially). This is possible because of the anisotropy of p_s, and the use of Eq. (2.6) leads to an underestimation of the fraction of particles that will run away. A more pertinent definition can be obtained by looking at particle trajectories in phase space [58]. The trajectory which terminates at $\xi = 1$ and $p = p_\mathrm{c}$ is the separatrix, since particles on it neither end up in the bulk population nor reach arbitrarily high energies. This trajectory is given by [59]

$$p_\mathrm{s,traj}^2(\xi) = \left(\frac{\xi + 1}{2}\frac{E}{E_\mathrm{c}} - 1\right)^{-1}. \tag{2.7}$$

The two separatrices in a typical scenario are shown in Fig. 2.3. In many cases, the runaways form a narrow beam close to the parallel axis, in which case p_s and $p_\mathrm{s,traj}$ give similar results. In fact, in these cases an isotropic runaway region ($p_\mathrm{s,iso}(\xi) = p_\mathrm{c}$) also is a good approximation (as discussed in Paper C),

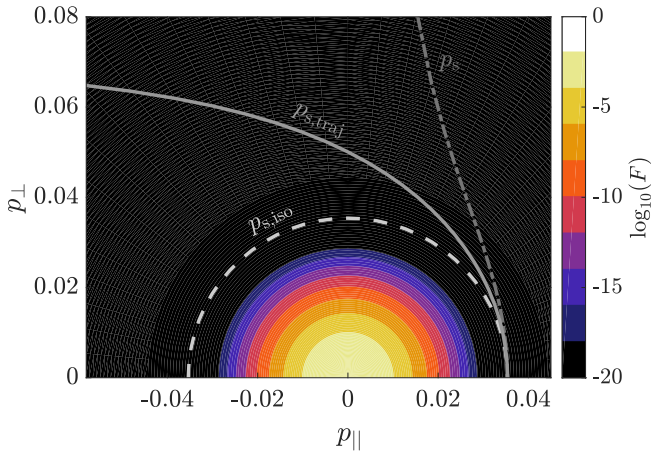

Figure 2.3: Runaway-region separatrices p_{s}, $p_{\mathrm{s,traj}}$ and $p_{\mathrm{s,iso}}$ at an electric field $E/E_{\mathrm{c}} = 800$, overlayed on contours of a Maxwellian distribution with $T_{\mathrm{e}} = 5.1\,\mathrm{eV}$ and $n_{\mathrm{e}} = 5 \cdot 10^{19}\,\mathrm{m}^{-3}$. F is the distribution f normalized to its maximum value ($F = f/\max[f]$).

and such a separatrix has been included in the figure as well. In certain cases, such as when hot-tail generation dominates (see Sec. 2.2.2), the details of the separatrix are however of importance for the size of the runaway population.

The separatrices discussed so far are valid in the limit where the bulk of the distribution is well described by a nonrelativistic Maxwellian, and when including only friction due to Coulomb collisions. As is suggested by the results in Paper D, however; synchrotron radiation reaction may have a significant impact on the separatrix (see also Refs. [60–62]).

In general, the separatrix for an arbitrary electron distribution can be obtained by considering the forces that affect a test particle:

$$\frac{\mathrm{d}p}{\mathrm{d}t} = F^p_{\mathrm{E}} - F^p_{\mathrm{C}} - F^p_{\mathrm{Syn}}, \tag{2.8}$$

$$\frac{\mathrm{d}\xi}{\mathrm{d}t} = F^\xi_{\mathrm{E}} - F^\xi_{\mathrm{C}} - F^\xi_{\mathrm{Syn}}, \tag{2.9}$$

where the expressions for the force associated with the electric field, F^i_{E} (with $i \in \{p, \xi\}$), and the synchrotron radiation-reaction force F^i_{Syn} are discussed in

Sec. 3.1 and Sec. 4.2, respectively. The expressions for the collisional electron-electron friction F_{C}^{i} are given in Paper E (see also Sec. 5.1 of that paper). Although other reaction forces (such as bremsstrahlung) may also contribute to the force balance, here we include only the synchrotron radiation-reaction force as it is the dominant contribution in most plasmas of interest. The critical momentum in the parallel direction can be determined from $\mathrm{d}p/\mathrm{d}t = 0$ at $\xi = 1$, since the separatrix becomes purely perpendicular to the parallel axis as $\xi \to 1$. The separatrix can then be traced out by numerically integrating the above equations from $\xi = 1$ to $\xi = -1$. In the appropriate limit, the result agrees with $p_{\mathrm{s,traj}}(\xi)$. In general, the separatrix depends on the distribution through the terms F_{C}^{i} and should be updated as the distribution changes.

It should be noted that in certain situations, additional regions in momentum space emerge which cannot be characterized as either bulk or runaway regions. The example of bump-on-tail formation induced by synchrotron or bremsstrahlung emission, where relativistic electrons accumulate around a certain multi-MeV energy, is discussed in Papers G, H and I (not included in the thesis). The momentum space dynamics leading to the formation of the bump is complicated and involves the interaction between acceleration, pitch-angle scattering and subsequent synchrotron or bremsstrahlung emission back-reaction, forming structures akin to convection cells in the high-energy electron distribution [Paper H]. Such phenomena are not described by the above definition for the separatrix (although generalized models exist that do take them into account, see for instance [60, 63]).

2.2 Runaway-generation mechanisms

There are two main mechanisms for generating runaways, referred to as *Dreicer* [1, 2] and *avalanche* [50, 64–66] generation. In the former, initially thermal electrons become runaways by a gradual diffusion through momentum space until they reach a velocity where they run away. Dreicer generation is an example of a *primary* mechanism, as it generates runaways without the need for a pre-existing fast population. Once some runaways exist, one of them may impart a large fraction of its momentum to a thermal electron in a single event, known as a *knock-on* collision. This generates a second runaway if both electrons are in the runaway region after the collision. This process is also called *secondary* runaway generation, as it requires the presence of a seed, and leads to an exponential growth of the runaway population (hence the name avalanche). In this section, we will look more closely at these two

mechanisms. We will also discuss another primary runaway mechanism: *hot-tail* generation, which can dominate if the plasma temperature decreases on a short timescale.

2.2.1 Dreicer generation

Due to momentum-space transport processes, new particles steadily diffuse into the runaway region, increasing the runaway density. This is known as *Dreicer generation*, and is caused by the gradient $\partial f/\partial p$ that develops across the separatrix as particles in the runaway region are accelerated to higher energies. An approximate expression [56, 67–69] for the steady-state growth rate of the runaway population due to this effect is

$$\frac{\mathrm{d}n_\mathrm{r}}{\mathrm{d}t} = C n_\mathrm{e} \nu_\mathrm{th}\, \epsilon^{-3(1+Z_\mathrm{eff})/16} \exp\left[-\frac{1}{4\epsilon} - \sqrt{\frac{1+Z_\mathrm{eff}}{\epsilon}}\right], \tag{2.10}$$

where $\epsilon = E/E_\mathrm{D}$, n_r is the runaway number density,

$$\nu_\mathrm{th} = \frac{n_\mathrm{e} e^4 \ln\Lambda}{4\pi\varepsilon_0^2 m_\mathrm{e}^2 v_\mathrm{th}^3} \tag{2.11}$$

is the electron-electron collision frequency of thermal particles, C is a constant of order unity [4, 56] (not determined by the analytical model), and Z_eff is the effective ion charge, which is a measure of the plasma composition ($Z_\mathrm{eff} = 1$ is a plasma consisting of pure hydrogen, or otherwise singly charged ions). Equation 2.10 is valid when the distribution is close to a Maxwellian, i.e. when ϵ is small; and for $E \gg E_\mathrm{c}$. Closer to the critical field, correction factors are introduced in the exponents so that the growth rate vanishes for $E \leq E_\mathrm{c}$ [56], but these are neglected here for simplicity.

Note that the growth rate depends on (and is exponentially small in) E/E_D, not E/E_c. This means that even if the field is significantly larger than E_c, the runaway production rate may be very small if $E \ll E_D$. This effect, which is in essence a temperature dependence, can partly explain recent observations indicating that $E/E_\mathrm{c} \gtrsim 10$ is required for runaway acceleration [41, 42]. Its importance is discussed and quantified in Paper D.

2.2.2 Hot-tail generation

Primary runaways can also be produced by processes other than momentum-space diffusion, for instance by highly energetic γ-rays through pair produc-

tion, or in tritium decay (in fusion plasmas). In a typical fusion plasma, these two processes are usually insignificant, however if the conditions are right they may provide a sufficient seed for avalanche multiplication [70]. There is however an additional primary-runaway mechanism – *hot-tail* generation [47, 71] – which relies on a rapid cooling of the plasma. If the plasma-cooling timescale is significantly shorter than the collision time at which particles equilibrate, electrons that initially constituted the high-energy part of the bulk distribution can remain as a drawn-out tail at the new lower temperature. This is because they take a longer time to equilibrate, as their collision time is significantly longer than that of the slow particles. If an electric field is also present, some of these tail electrons may belong to the runaway region of momentum space and will therefore be accelerated.

Under certain circumstances, hot-tail generation can be the dominating runaway-generation mechanism – albeit for a short time – and may provide a strong seed for multiplication by the avalanche mechanism. This is particularly the case in disruptions in tokamaks, where the plasma quickly loses essentially all stored thermal energy due to a sudden degradation in confinement. Approximately, hot-tail generation dominates over Dreicer generation in a disruption if

$$\nu_{\mathrm{th},0}\, t_{\mathrm{T}} < \frac{1}{3}\left(\frac{3\sqrt{\pi}}{4}\frac{\mu_0 e n_{\mathrm{e}} v_{\mathrm{th,f}}\, q_{\mathrm{a}} R}{B_{\mathrm{a}}}\right)^{3/2} \tag{2.12}$$

is fulfilled [59], where $\nu_{\mathrm{th},0}$ is the initial thermal collision frequency, t_{T} is the temperature-decay time, μ_0 is the vacuum permeability, $v_{\mathrm{th,f}}$ is the thermal speed at the final temperature, R is the major radius of the tokamak, and B_{a} and q_{a} are the magnetic field and so-called *safety factor* [20] on its magnetic axis. This estimate was obtained by assuming the temperature drop to be described by $T_{\mathrm{e}}(t) = T_{\mathrm{e},0}(1 - t/t_{\mathrm{T}})^{2/3}$, with $T_{\mathrm{e},0}$ the initial temperature.

The hot-tail mechanism is discussed in Paper C. See also Refs. [59, 72–74] for a more in-depth discussion of hot-tail growth rates in various cooling scenarios.

2.2.3 Secondary generation

Secondary runaways are formed when existing runaways collide with thermal electrons, if the collision imparts enough momentum to the thermal electron to kick it into the runaway region while the incoming (primary) electron remains a runaway itself [50, 64–66]. Such events are referred to as *close*, *large-angle* or

knock-on collisions, and are normally rare in a fusion plasma (their contribution to the collisional dynamics is a factor $\ln\Lambda$ smaller than that of small-angle collisions). In the context of runaway generation they become important due to the special characteristics of the runaway region, since once a particle is a runaway it can quickly gain enough energy to cause knock-on collisions of its own. For it to be able to contribute to the avalanche process, the kinetic energy of the incoming runaway must be at least twice as large as the critical energy: $\gamma - 1 > 2(\gamma_\mathrm{c} - 1)$.

The avalanche growth rate was calculated by Rosenbluth & Putvinski [50], who also derived an approximate operator for avalanche generation (see Paper C and Sec. 3.3 for a detailed discussion of avalanche operators and their influence on runaway dynamics). In a cylindrical plasma, the growth rate takes the form

$$\frac{\mathrm{d}n_\mathrm{r}}{\mathrm{d}t} \simeq n_\mathrm{r}\nu_\mathrm{rel}\,\frac{(\mathcal{E}-1)}{c_\mathrm{z}\ln\Lambda}\left(1-\mathcal{E}^{-1}+\frac{4(Z_\mathrm{eff}+1)^2}{c_\mathrm{z}^2(\mathcal{E}^2+3)}\right)^{-1/2}, \tag{2.13}$$

where $\mathcal{E} = E/E_\mathrm{c}$ and $c_\mathrm{z} = \sqrt{3(Z_\mathrm{eff}+5)/\pi}$. In the limit where $E \gg E_\mathrm{c}$ and $Z_\mathrm{eff} = 1$, this simplifies to

$$\frac{\mathrm{d}n_\mathrm{r}}{\mathrm{d}t} \simeq \sqrt{\frac{\pi}{2}}\,n_\mathrm{r}\nu_\mathrm{rel}\,\frac{(\mathcal{E}-1)}{3\ln\Lambda}\,. \tag{2.14}$$

The growth rate is proportional to the runaway density n_r, meaning that the growth is exponential (hence the name avalanche). We also note that the dependence on E is linear in Eq. (2.14), and nearly so in the more general expression (2.13), whereas it is exponential in Eq. (2.10) for the Dreicer growth rate. Therefore, avalanche generation tends to dominate for weak fields (as long as there is some runaway population to start with), but for strong fields primary generation becomes more important.

2.3 Damping and loss mechanisms for runaways

The discussion so far has focused on the interplay between the electric field and elastic Coulomb collisions in a quiescent, homogeneous, fully ionized plasma. In practice, runaway electrons do not reach arbitrarily high energies or persist indefinitely. Many processes contribute to the damping of their growth, slowing them down, or transporting them out of the plasma.

Of particular importance when it comes to limiting the energy achieved by the runaways are radiative processes: synchrotron-radiation emission due to

(predominantly) the gyro motion, and fast-electron bremsstrahlung due to inelastic scattering off the much heavier ions. The emitted radiation takes away momentum, and the electron must therefore lose a corresponding amount. This radiation reaction effectively introduces an additional force which can counteract the accelerating electric field. Synchrotron radiation is discussed in more detail in Chapter 4 and the effect of bremsstrahlung emission was studied in Paper G.

Another factor that can increase the effective friction compared to the classical estimate is partially ionized atoms. The highly energetic runaway electrons may penetrate (parts of) the electron cloud surrounding the nucleus and thus effectively scatter off a charge larger than the net charge of the ion. For heavy ions such as argon or tungsten, which are often present during or after disruptions, this can have a significant effect on the runaway slowing-down [75–79]. The runaways may also lose energy in ionizing collisions.

The above mechanisms are pure momentum-space effects. The runaway beam will however eventually occupy a sizable fraction of the tokamak cross-section, and magnetic trapping effects may become important. They typically lead to a reduction in both the Dreicer and avalanche growth rates, which can be as large as 50% already at $r/R = 0.1$, with r and R the minor and major radii [46]. Additionally, stochastic field-line regions (caused by for instance overlapping magnetic-island structures) can lead to radial transport of the runaways towards the edge of the plasma, where they are eventually lost to the wall [49]. This can be both beneficial (if it occurs early in the acceleration process, before the runaways have reached high energies) and detrimental (if a fully formed, substantial runaway beam is transported into the wall). By applying external magnetic fields with a well-defined periodicity, so-called Resonant Magnetic Perturbations (RMPs), the stochasticity of the edge region of the plasma can be purposefully increased. This can lead to a more rapid radial transport of the runaways, resulting in a reduction in their kinetic energy upon impact with the wall, however since the runaways predominantly form in the center of the plasma, efficient mitigation can be hard to achieve [80–82].

The runaways are also subject to outward radial transport because of another, more fundamental effect: the acceleration of a runaway particle implies a change in its angular momentum with respect to the symmetry axis of the torus. This causes a shift of the runaway orbit away from the flux surface, as the canonical angular momentum of the particle should be conserved [83, 84].

At high enough particle energies, the runaways will simply drift out of the plasma and into the wall.

Another effect not captured by a pure momentum-space treatment is the interaction of the runaways with various waves in the plasma. There is evidence that existing waves, such as toroidal Alfvén eigenmodes, can disperse the runaway beam [85–88]. Due to their highly anisotropic momentum distribution, the runaways may also destabilize and act as a drive for plasma waves, such as the whistler [89–91] and EXtraordinary ELectron (EXEL) waves [92, Paper K], which in turn can affect the runaway distribution and reduce the runaway growth.

The picture is thus complicated in practice, however even the basic dynamics of the runaway process are not always well understood. Significant experimental and theoretical effort is spent on improving that understanding and it is the aim of this thesis to contribute to this endeavor.

3 Simulation of runaway-electron momentum-space dynamics

Although the single-particle estimates considered in Chapter 2 can be useful in describing some of the phenomena associated with runaways, a complete and thorough understanding of their dynamics can only be gained through a treatment of the full kinetic problem. In some idealized situations the equations can be solved analytically, however in general the interplay between the various processes involved in the momentum-space transport of electrons must be studied using numerical tools.

The runaways often comprise a small fraction of the total number of electrons, and features in the distribution of electrons many orders of magnitude smaller than the bulk population must be accurately resolved. Continuum discretization methods (i.e. finite difference, element, and volume methods) are well adapted for problems of this type, whereas Monte Carlo methods become inefficient and have problems with numerical noise. In this thesis, two finite-difference tools for studying runaway-electron dynamics are described: `CODE` (Papers B and C, Sec. 3.4) and `NORSE` (Paper E, Sec. 3.5). Microscopic Coulomb interaction between particles (collisions) are very important for the runaway dynamics and we will discuss the treatment of both small (Sec. 3.2) and large-angle (Sec. 3.3) collisions. Another important effect is synchrotron radiation reaction, however we postpone the description of the corresponding operator to Sec. 4.2.3.

We begin by discussing the equations governing the evolution of the electron population.

3.1 The kinetic equation

When it comes to describing plasma phenomena, several theoretical frameworks of varying degrees of complexity (and explanatory power), have been

developed. Fluid theories, although tractable, numerically efficient, and useful in other contexts, are based on the assumption that the plasma particles are everywhere in local thermal equilibrium and can be described by near-Maxwellian distributions. In order to treat the runaway-electron phenomenon, such a model is inadequate[1], as the runaways by definition constitute a high-energy (non-thermal) tail of the particle distribution. It is therefore necessary to use *kinetic theory*, where the distribution of particle positions and velocities is the prime object of study.

The so-called *kinetic equation* describes the evolution of a distribution of plasma particles of species a, $f_a(\mathbf{x}, \mathbf{p}, t)$, according to

$$\frac{\partial f_a}{\partial t} + \frac{\partial}{\partial \mathbf{x}} \left(\dot{\mathbf{x}} f_a \right) + \frac{\partial}{\partial \mathbf{p}} \left(\dot{\mathbf{p}} f_a \right) = \sum_b C_{ab}\{f_a, f_b\} + S, \tag{3.1}$$

where $\mathbf{x}$ and $\mathbf{p}$ denote the position and momentum, respectively, and $\dot{\mathbf{p}}$ describes the macroscopic equations of motion (given for instance by the Lorentz force due to the presence of macroscopic electric and magnetic fields). The *collision operator* C_a describes microscopic interactions between the plasma particles (collisions), which are normally treated separately from the macroscopic equations of motion. In general, the collision operator depends on the distributions of all the particle species b in the plasma and includes contributions from both elastic and inelastic Coulomb collisions. In the latter (which are often neglected), photons are emitted and carry away some of the energy and momentum – this radiation is referred to as bremsstrahlung (see for instance Paper G). S represents any sources or sinks of particles or heat, such as ionization and recombination of neutral atoms, fueling in laboratory plasmas or heat lost from the plasma, due to radiative processes.

Under certain conditions, the collisions can be neglected, in which case Eq. (3.1) (with $S = 0$) is known as the *Vlasov equation.* With a two-particle collision operator valid for arbitrary momentum transfer (or equivalently collision distance), it is called the *Boltzmann equation,* although in practice several simplifications must be made to be able to treat the collisions. Under the assumption that the momentum transfer in each collision is small, the Boltzmann collision operator simplifies to the Fokker-Planck collision operator, and Eq. (3.1) is correspondingly called the *Fokker-Planck equation* [93, 94]. This operator is sufficient to treat primary runaway generation, but is not able to describe the

[1] Interestingly, in his seminal papers on electron runaway, Dreicer derived the basic runaway dynamics using a two-fluid treatment [1]. He did however recognize the limitations of this description and the follow-up paper uses a kinetic approach [2].

avalanche process in which the momentum transfer to the secondary particle in a knock-on collision is significant. Avalanche generation is instead treated by including a special source term S_{ava}, discussed in Sec. 3.3.

In general, the distribution f_a is defined on a six-dimensional phase-space, and is very demanding to treat in its entirety. Various approximations are routinely employed to reduce the kinetic equation to a manageable number of dimensions (see for instance Ref. [54]). In many situations, the fundamentals of the runaway problem can be studied in a homogeneous plasma, so that the spatial dependence can be ignored. In addition, one of the momentum-space dimensions (describing the rapid gyro motion around the magnetic field lines) can be averaged over if a sufficiently strong magnetic field is present (so that the gyro radius is ignorable in comparison to the typical length scale of the gradients in the plasma and the gyration time is short compared to the timescales of other processes). The tools developed here therefore solve the kinetic equation in two momentum-space dimensions only, allowing for fast calculation while most of the relevant physics is retained.

The kinetic equation implemented in `CODE` and `NORSE` can be expressed as

$$\frac{\partial f_{\mathrm{e}}}{\partial t} - \frac{e\mathbf{E}}{m_{\mathrm{e}}c}\cdot\frac{\partial f_{\mathrm{e}}}{\partial \mathbf{p}} + \frac{\partial}{\partial \mathbf{p}}\cdot(\mathbf{F}_{\mathrm{syn}} f_{\mathrm{e}}) = C_{\mathrm{ee}}\{f_{\mathrm{e}}\} + C_{\mathrm{ei}}\{f_{\mathrm{e}}\} + S_{\mathrm{ava}} + S_{\mathrm{p}} + S_{\mathrm{h}}, \quad (3.2)$$

where the second term describes the acceleration due to the electric field, the third term describes the effects of synchrotron radiation reaction (see Sec. 4.2), C_{ee} and C_{ei} describe collisions with electrons and ions, respectively, and S_{p} and S_{h} are sources of particles and heat. The two momentum-space dimensions are conveniently described by the coordinates (p, ξ) introduced in Sec. 2.1.3. In these coordinates, the electric-field term becomes

$$\frac{e\mathbf{E}}{m_{\mathrm{e}}c}\cdot\frac{\partial f_{\mathrm{e}}}{\partial \mathbf{p}} = \frac{eE_{\parallel}}{m_{\mathrm{e}}c}\left(\xi\frac{\partial f_{\mathrm{e}}}{\partial p} + \frac{1-\xi^2}{p}\frac{\partial f_{\mathrm{e}}}{\partial \xi}\right). \quad (3.3)$$

Equation (3.2) is then solved for the electron distribution. Both `CODE` and `NORSE` can calculate the time evolution of f_e, starting from some initial (often Maxwellian) distribution, and `CODE` is also able to determine the (quasi) steady-state distribution directly (in the absence of an avalanche source). In general, parameters such as the electric field, effective charge, temperature, and density may vary in time, and both tools have the ability to model this. Such capability is necessary in order to describe hot-tail runaway generation and other dynamic scenarios.

Throughout the rest of this thesis, we will omit the subscript e, and let f denote the distribution function of electrons. We will also assume an implicit minus sign in the electric field, so that the runaway electrons are accelerated in the positive-p direction.

The evolution of the distribution function in a typical runaway case is shown in Fig. 3.1. Starting from a Maxwellian distribution, the electric field pulls out a high-energy tail centered around $p_\perp = 0$ (but with significant spread in $p_\perp$ due to pitch-angle scattering). In 500 thermal collision times, the tail of the distribution reaches $p_\parallel \approx 8$, which corresponds to a kinetic energy of 3.6 MeV.

3.2 Collision operator

As discussed in the previous section, the two tools `CODE` and `NORSE` have many of the same capabilities. The main difference between them lies in the treatment of the electron-electron Coulomb collisions. `CODE` uses a collision operator linearized around a Maxwellian, taking advantage of the fact that the runaways in many cases constitute a small part of the electron distribution, so that the collisions between runaways may be neglected. This approach allows for very efficient numerical evaluation of the problem as long as the plasma parameters remain constant. `NORSE`, on the other hand, uses a fully nonlinear relativistic collision operator [95–97], which makes it possible to treat distributions of arbitrary shape. Thus, `NORSE` can be used in situations where the runaways make up a sizable fraction of the distribution, or where the electric field is strong enough that the electron population is in the slide-away regime ($E > E_{\mathrm{sa}}$). For a thorough discussion of collision operators in general, see Ref. [54].

The generally valid collision operator in `NORSE` accurately treats the elastic electron-electron collisions in the Fokker-Planck limit. However, in the linearization procedure used to derive the operator in `CODE`, some properties of the full operator are compromised. In particular, the linearized operator is often written as a sum of so-called *test-particle* and *field-particle* terms:

$$C_{\mathrm{ee}}\{f\} \simeq C^{\mathrm{l}}_{\mathrm{ee}}\{f\} = C^{\mathrm{tp}}_{\mathrm{ee}} + C^{\mathrm{fp}}_{\mathrm{ee}}, \tag{3.4}$$

where the test-particle term $C^{\mathrm{tp}}_{\mathrm{ee}} = C_{\mathrm{ee}}\{f_1, f_{\mathrm{M}}\}$ describes collisions of the perturbation f_1 with the bulk plasma (f_{M}), and the field-particle term $C^{\mathrm{fp}}_{\mathrm{ee}} = C_{\mathrm{ee}}\{f_{\mathrm{M}}, f_1\}$ describes the reaction of the bulk to the perturbation. Here, $f = f_{\mathrm{M}} + f_1$ with $f_1 \ll f_{\mathrm{M}}$, and thus collisions between particles represented

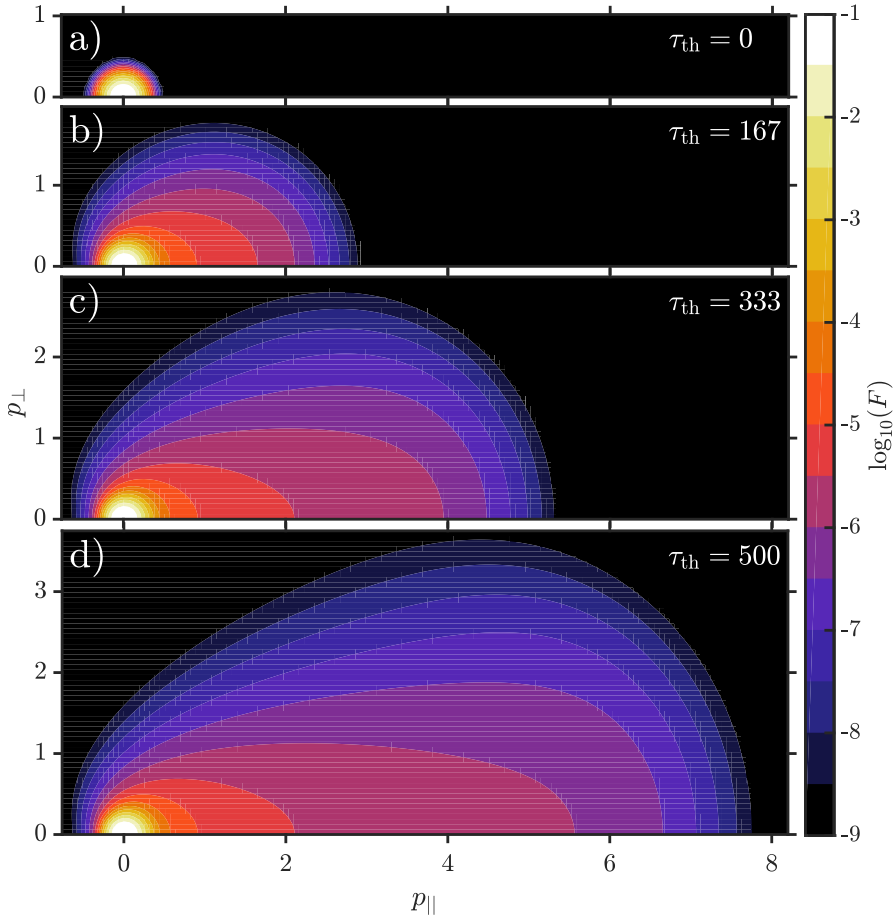

Figure 3.1: Evolution of the electron distribution under a constant electric field of $E = 0.4\,\mathrm{V/m}$ (corresponding to $E/E_\mathrm{c} = 9.6$ and $E/E_\mathrm{D} = 0.056$). Contours of the distribution ($F = f/\max[f]$) in 2D momentum space are shown at a) the initial time, b) $\tau_\mathrm{th} = 167$, c) $\tau_\mathrm{th} = 333$, and d) $\tau_\mathrm{th} = 500$ thermal collision times. The parameters were: $T = 3\,\mathrm{keV}$, $n = 5 \cdot 10^{19}\,\mathrm{m}^3$, $Z_\mathrm{eff} = 2$ and $B = 0$, and the results were obtained using `CODE` with avalanche generation disabled.

by the perturbation ($C_{\mathrm{ee}}\{f_1, f_1\}$) have been neglected as they are second order in the small quantity f_1.[2] It is common in runaway studies to neglect the field-particle term, as it only affects the bulk plasma and complicates the problem. If this is done, however, the conservation properties of the linearized operator $C^{\mathrm{l}}_{\mathrm{ee}}$ are compromised as the test-particle term only conserves particles, not momentum or energy. This does not significantly affect the runaway dynamics, but is important for the accurate determination of properties of the bulk (such as the conductivity). CODE includes both test-particle and field-particle terms, as discussed in Paper C, however unlike in NORSE, the latter term is nonrelativistic (i.e. the bulk temperature is assumed to be small compared to the electron rest energy). The test-particle term in CODE, which is valid for arbitrary energies, was derived in Ref. [80].

Electron-ion collisions can be described by a much simpler operator, due to the mass difference between the species involved in the collision (and assuming the ions to be immobile on the timescales of interest). Both CODE and NORSE use an electron-ion collision operator which describes pitch-angle scattering, but neglects the energy transfer to the much heavier ion [54].

As part of the work on Paper G (not included in this thesis), an operator for inelastic (bremsstrahlung) Coulomb collisions was developed, and is available in CODE [98].

3.3 Avalanche source term

The avalanche process due to large-angle Coulomb collisions between existing runaways and thermal electrons cannot be captured using the Fokker-Planck formalism, and a special source term – derived from the Boltzmann collision operator – must be included to treat this process. In a linearized formulation, several avalanche sources describing the creation of the secondary runaway particles can be formulated (using various assumptions, as will be discussed shortly), however in the case of a strongly non-Maxwellian distribution function f, no such easily tractable operator is available. For this reason, the avalanche operators described below are included in CODE but not in NORSE.

[2] Note that for the runaway problem, it is not required that $f_1(p,\xi) \ll f_{\mathrm{M}}(p,\xi)$ for all p and ξ – only that the perturbation is small in a global sense, so that collisions between runaway particles can be ignored. In the tail, the perturbation is usually many orders of magnitude larger than the Maxwellian at the corresponding momentum.

The generally-valid Boltzmann collision operator is notoriously difficult to handle numerically, and an efficient solution of the runaway problem requires the use of reduced models. Work on a simplified conservative treatment of the avalanche process is ongoing [Conf. Contrib. S], but no practical such operator is yet available. From the kinematics of a single large-angle collision, a source term for the generated secondary particles can however be derived, taking the energy distribution of the incoming electrons into account by utilizing the full Møller scattering cross-section [99]. This was demonstrated by Chiu *et al.* in 1998 [47]. This operator obeys the kinematics of the problem (in the sense that the momentum of the generated particle is restricted by that of the incoming particle), however since no sink of particles is included, it violates the conservation properties of the full Boltzmann operator. No modification to the momentum of the incoming particle is made and no particle is removed from the thermal population. Nevertheless, the operator in Ref. [47] is able to accurately capture the exponential growth of the avalanche. The source term at a point (p,ξ) takes the form

$$S_{\mathrm{Ch}}(p,\xi) = \frac{1}{2}\frac{\nu_{\mathrm{rel}}}{\ln\Lambda}\frac{p_{\mathrm{in}}^4 \tilde{f}(p_{\mathrm{in}})\Sigma(\gamma,\gamma_{\mathrm{in}})}{\gamma p \xi}, \tag{3.5}$$

where p_{in} and γ_{in} are the normalized momentum and relativistic mass factor of the incoming primary runaway, γ is the relativistic mass factor for the generated secondary runaway, $\tilde{f}$ is the angle-averaged electron distribution (i.e. all incoming particles are assumed to have vanishing pitch-angle), and Σ is the Møller cross section. Note that due to the kinematics of the problem, the coordinates are related in such a way that only primary particles with a single p_{in} can contribute to the source at a point (p,ξ).

By taking the high-energy limit of the Møller cross section, i.e. assuming that the incoming primaries are all highly relativistic, the source term can be simplified further. The resulting operator, first derived by Rosenbluth and Putvinski the year before [50], is widely used and given by

$$S_{\mathrm{RP}}(p,\xi) = \frac{n_{\mathrm{r}}}{4\pi}\frac{\nu_{\mathrm{rel}}}{\ln\Lambda}\delta(\xi-\xi_{\mathrm{s}})\frac{1}{p^2}\frac{\partial}{\partial p}\left(\frac{1}{1-\gamma}\right). \tag{3.6}$$

Due to the assumptions used, the kinematics are restricted further, and all secondary runaways are generated on a parabola given by $\xi_{\mathrm{s}} = p/(1+\gamma)$. However, since every runaway is assumed to have very large momentum, secondary particles can be generated with momenta larger than that of any of the particles in the actual distribution. This is illustrated in Fig. 3.2, where

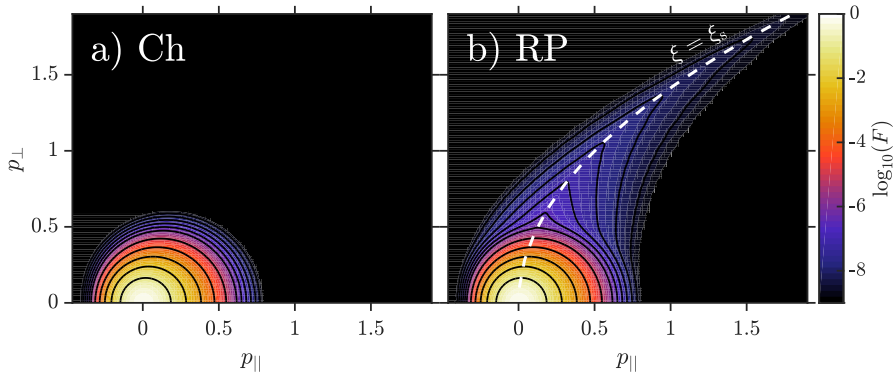

Figure 3.2: Electron distribution ($F = f/\max[f]$) after 10 thermal collision times with a) the source in Eq. (3.5) and b) the source in Eq. (3.6). This early in the evolution, the result with only primary generation included is indistinguishable from that in a). The parameters were: $T = 300\,\mathrm{eV}$, $n = 5 \cdot 10^{19}\,\mathrm{m}^3$, $E = 0.5\,\mathrm{V/m}$ (corresponding to $E/E_\mathrm{c} = 12$ and $E/E_\mathrm{D} = 0.07$), $Z_\mathrm{eff} = 1$ and $B = 0$, and the results were obtained using `CODE`.

an unphysical horn-like structure is created, extending to large momenta. In some situations, the Rosenbluth-Putvinski model therefore tends to overestimate the avalanche growth rate, compared to the source term of Chiu *et al.* However, as is shown in Paper C; in certain parameter regimes, the opposite tendency is seen. This is due to the non-trivial dependence of the Møller cross section on the momenta of the colliding particles.

If secondary generation dominates, the quasi-steady-state runaway distribution function can be calculated analytically (assuming a growth rate consistent with the Rosenbluth–Putvinski source), and is given by

$$f_\mathrm{ava}(p_\parallel, p_\perp) = \frac{n_\mathrm{r}\hat{E}}{\pi c_\mathrm{z} p_\parallel \ln\Lambda} \exp\left(-\frac{p_\parallel}{c_\mathrm{z}\ln\Lambda} - \hat{E}\frac{p_\perp^2}{p_\parallel}\right), \tag{3.7}$$

where $\hat{E} = (E/E_\mathrm{c} - 1)/2(1 + Z_\mathrm{eff})$ and $c_\mathrm{z} = \sqrt{3(Z_\mathrm{eff} + 5)/\pi}$ [89]. Equation (3.7), which is valid when $\gamma \gg 1$ and $E/E_\mathrm{c} \gg 1$, was used extensively in the calculation of synchrotron spectra in Paper A, and also as a benchmark in Paper B. An example distribution is plotted in Fig. 3.3.

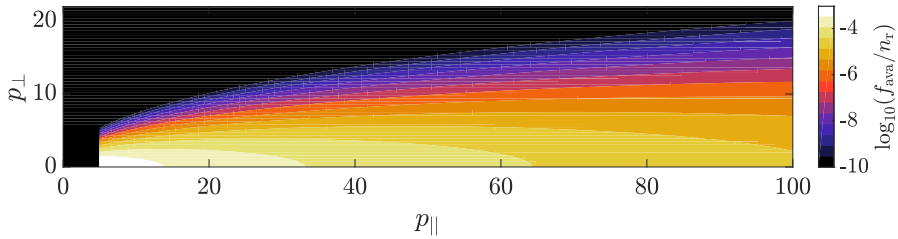

Figure 3.3: Contour plot of the tail of the analytical avalanche distribution in Eq. (3.7) for $T_\mathrm{e} = 1$ keV, $n_\mathrm{e} = 1 \cdot 10^{20}$ m^{-3}, $Z_\mathrm{eff} = 1.5$ and $E/E_\mathrm{c} = 15$. The distribution is not valid for the bulk plasma, and is therefore cut off at low momentum (in this case at $p_\parallel = 5$).

3.4 CODE

CODE (COllisional Distribution of Electrons) was developed to be a lightweight tool dedicated to the study of the properties of runaway electrons. It solves the kinetic equation (3.2) using a finite-difference discretization of p together with a Legendre-mode decomposition of ξ, and an implicit time-advancement scheme. The discretization is advantageous as the Legendre polynomials are eigenfunctions of the collision operator, allowing for a straight-forward implementation and an efficient numerical treatment. In particular, time advancement can be performed at low computational cost, as it is sufficient to build and invert the matrix representing the system only once, provided that the plasma parameters are independent of time. The system can then be advanced in time using just a few matrix operations in each time step. For small to moderately-sized problems, such as the scenario considered in Fig. 3.1, CODE runs in a couple of seconds on a standard desktop computer. More involved set-ups involving time-dependent plasma parameters or low temperatures in combination with large runaway energies execute in minutes or sometimes hours. Memory requirements range from a few hundred MB (or less) to tens of GB, depending on resolution. CODE, which is written in Matlab, has contributed to a number of studies and is used at several fusion sites around the world.

The original version, described in Paper B, included the relativistic test-particle collision operator [80] and the Rosenbluth-Putvinski avalanche operator in Eq. (3.6), as well as the ability to find both time-dependent and steady-state solutions for f. Subsequent extensions include: time-dependent

plasma parameters, the field-particle term of the collision operator and an associated heat sink, the Chiu *et al.* avalanche operator (all described in Paper C), and operators for synchrotron (Paper D, Sec. 4.2.3) and bremsstrahlung (Paper G) radiation reaction. Various other technical features, such as efficient non-uniform automatically extending finite-difference grids, have also been added [Conf. Contrib. V].

3.5 NORSE

Building on the experience gained from the work on `CODE`, `NORSE` (NOnlinear Relativistic Solver for Electrons) was developed to extend the range of applicability of runaway-modeling tools to the regime where the runaway population becomes substantial; i.e. the regime of greatest concern in practice. The fully nonlinear treatment also makes it possible to consistently study phenomena such as heating by the electric field, which is discussed in Paper F and Sec. 5.1.

The numerical implementation of `NORSE` – described in detail in Paper E – differs substantially from that in `CODE`. In particular, a linearly implicit time-advancement scheme is used to treat the nonlinear problem. The electron-electron collision operator implemented in `NORSE` is formulated in terms of five potentials (analogous to the two so-called Rosenbluth potentials [94] in the nonrelativistic case), which are functions of the distribution [96, 97]. By calculating the potentials explicitly in each time step from the known distribution, the remainder of the kinetic equation can be formulated as a matrix equation, which can be solved implicitly using standard techniques. Unlike in `CODE`, this scheme requires the formation and inversion of a matrix in each timestep, and is therefore in general more computationally demanding. If time-dependent parameters are used, however; `NORSE` is marginally faster than `CODE` due to an improved numerical implementation.

`NORSE`, also written in Matlab, uses a discretization scheme different to that in `CODE`, as required by the nonlinear problem. Momentum space is discretized on a two-dimensional non-uniform finite-difference grid, which allows for improved numerical efficiency as the grid points can be chosen in a way suited to the problem at hand (i.e. smaller grid spacing close to $\xi = 1$ where the runaway tail forms, but larger grid spacing around $\xi = 0$ where the distribution lacks fine-scale features). For the explicit calculation of the five potentials, however; a mixed finite-difference–Legendre-mode representation is employed (similar to `CODE`), as in this basis the potentials become one-dimensional in-

tegrals over p. This representation is only used to calculate the potentials – which are integral moments of f – and a small number of Legendre modes are often sufficient for an accurate treatment. The mapping between the two representations can be performed to machine precision at little computational cost.

NORSE includes time-dependent plasma parameters, an operator for synchrotron radiation reaction, a runaway region determined from the distribution in accordance with Eqs. (2.8) and (2.9), and elaborate heat and particle sinks.

4 Synchrotron radiation

Charged particles in accelerated motion emit radiation [100]. In the presence of a magnetic field, the particles in a plasma follow helical orbits as a consequence of the Lorentz force [21, 22]; in other words, they are continuously accelerated "inwards" – perpendicular to their velocities. The radiation emitted by electrons due to this motion is known as *cyclotron* radiation if the particles are nonrelativistic (or mildly so) and *synchrotron* or *betatron* radiation if they are highly relativistic (the names come from the types of devices where the radiation was first observed [101]). Synchrotron radiation has many applications in the study of samples in condensed matter physics, materials science, biology and medicine, where it is used in for instance scattering and diffraction studies, and for spectroscopy and tomography [102]. The radiation is usually produced using dedicated facilities (synchrotrons), but is also emitted in some natural processes, in particular in astrophysical contexts (where it can be used as a source of information about the processes in question).

From the distinction between cyclotron and synchrotron radiation, it is evident that in a nonrelativistic plasma (with a temperature significantly below 511 keV), only the far tail of the electron distribution may emit synchrotron radiation. The only plasma particles that reach highly relativistic energies are the runaway electrons; the study of the synchrotron emission from a plasma is thus a very important source of information about the runaways, and their dynamics.

Synchrotron radiation plays an important role in several of the papers included in this thesis. In Papers A and B, it is used as a source of information about the runaway population – as a "passive" diagnostic not affecting the electron distribution. This is discussed in Sec. 4.1. In Paper D (and also Papers H and I, not included in this thesis), the impact of the emission on the distribution is analyzed – i.e. the synchrotron radiation plays an "active" role through the radiation reaction associated with its emission, as discussed in Sec. 4.2.

4.1 Emission and power spectra

The theory of synchrotron radiation was first derived by Schott in 1912 [103], but was rediscovered, and to a large extent reworked, by Schwinger in the 40's [104]. More recent, detailed discussions of the properties of synchrotron radiation can be found in Refs. [100, 102, 105, 106]. In the rest frame of the particle, the synchrotron radiation is emitted almost isotropically, however the transformation to the lab frame introduces a strong forward-beaming effect. Since the motion of the particle is predominantly parallel to the magnetic field lines (the runaways are accelerated by $E_\parallel$), the synchrotron radiation will be emitted in this direction as well, even though it is the perpendicular motion of the particle that is the cause of the emission.

Since the synchrotron radiation is directed, its observation requires detectors in the right location and with the right field of view. In many tokamak experiments this necessitates the use of dedicated cameras for the study of synchrotron emission from runaways, and the number of such set-ups around the world is limited but has seen an increase in recent years. Synchrotron emission from runaways has now been observed in a number of tokamaks, including TEXTOR [107, 108], DIII-D [41, 109], ASDEX Upgrade [39], Alcator C-Mod [Conf. Contrib. L], FTU [110], EAST [111], KSTAR [25], and COMPASS [37].

Another important question is the emission spectrum, since it determines the detector type to use. As part of the work on Paper A, the numerical tool `SYRUP` (SYnchrotron emission from RUnaway Particles) was developed to calculate the synchrotron spectra of both single electrons and runaway distributions. As we shall see, the emission has a distinct peak; for runaways in tokamaks it is often located in the near infrared, at wavelengths of a few μm. Electrons with energies above about 20–25 MeV do however also emit a substantial amount of radiation in the visible range. The majority of the observations above were done using fast visual cameras, due to the availability and good performance of the technology compared to infrared detectors (although several IR systems are also in use). Visual cameras also provide a more sensitive diagnostic of the highest-energy part of the runaway distribution, which is often considered to be of most interest.

In this section, we will first examine the synchrotron spectra emitted by single electrons, followed by a generalization to a distribution of runaway electrons. This topic is also discussed in more detail in Paper A.

4.1.1 Single-particle spectrum in a straight magnetic field

The frequency of the cyclotron or synchrotron radiation emitted by a particle is a multiple of the frequency with which it orbits the magnetic field line (the *gyro* or *cyclotron* frequency $\omega_\mathrm{c} = eB/\gamma m_\mathrm{e}$). In the case of cyclotron emission, the fundamental and the first few harmonics dominate completely, whereas for the high-energy synchrotron emission, the high harmonics (up to some cut off) are dominant. Since these are spaced very close together (compared to the scale of the fundamental frequency), synchrotron radiation essentially has a continuous frequency spectrum [105]. The emission can span a large part of the electromagnetic spectrum, from microwaves to hard x rays, depending on the frequency of the gyro motion and the electron energy.

In terms of quantities convenient for plasma physics [105], the synchrotron power spectrum emitted by a fast electron can be expressed as

$$\mathcal{P}(\lambda) = \frac{1}{\sqrt{3}} \frac{ce^2}{\varepsilon_0 \lambda^3 \gamma^2} \int_{\lambda_c/\lambda}^{\infty} K_{5/3}(l)\,\mathrm{d}l \ , \tag{4.1}$$

where $K_\nu(x)$ is the modified Bessel function of the second kind (of order ν), and λ_c is a critical wavelength given by

$$\lambda_\mathrm{c} = \frac{4\pi}{3} \frac{c}{\omega_\mathrm{c} \gamma^3} = \frac{4\pi}{3} \frac{c m_\mathrm{e} \gamma_\parallel}{eB\gamma^2} \ , \tag{4.2}$$

with $\gamma_\parallel = (1 - v_\parallel^2/c^2)^{-1/2}$ the relativistic γ factor due to the motion parallel to the magnetic field, and B the magnetic field strength. The spectrum, which peaks at $\lambda \simeq 0.42\lambda_\mathrm{c}$, is plotted in Fig. 4.1 for a few different parameter sets. There is a sharp cutoff at short wavelengths, but a much slower decay towards longer wavelengths. Note that both the peak wavelength and the emitted power are sensitive to both the particle energy and pitch. In particular, it is possible to produce similar synchrotron spectra using significantly different parameter sets, which makes it difficult to treat the inverse problem of finding the parameters of a particle (or distribution) that produced a certain spectrum.

4.1.2 Single-particle spectrum in a toroidal magnetic field

Equation (4.1) considers the radiation emitted due to pure gyro motion around a straight field line. In a tokamak, particle orbits are more complicated since

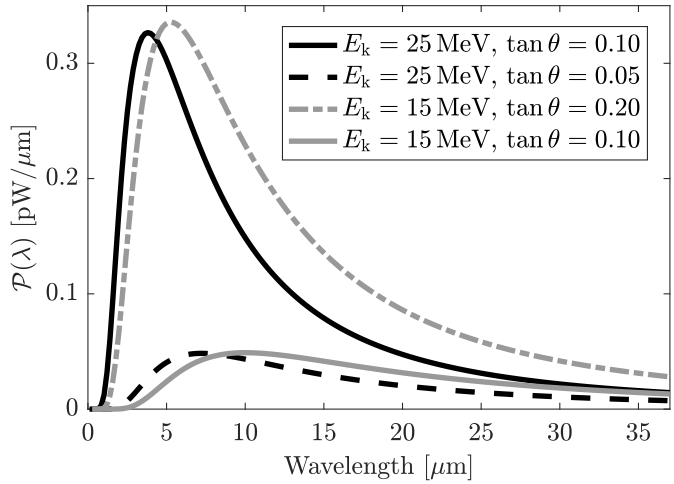

Figure 4.1: Synchrotron power spectrum for a single electron with kinetic energy E_k and pitch described by $\tan\theta = v_\perp/v_\parallel$ (with θ the pitch angle).

both the motion around the torus, that due to the helicity of the field lines, and various drifts contribute. The synchrotron power spectrum for a particle trajectory including the gyro motion, the motion along a toroidal magnetic field, and vertical centrifugal drift was derived by I. M. Pankratov in 1999 [112], and is

$$\mathcal{P}(\lambda) = \frac{ce^2}{\varepsilon_0 \lambda^3 \gamma^2} \left(\int_0^\infty g(y)\, J_0\left(a\zeta y^3\right) \sin\left(h(y)\right) \mathrm{d}y \right. \\ \left. -4a \int_0^\infty y\, J_0'\left(a\zeta y^3\right) \cos\left(h(y)\right) \mathrm{d}y \; - \; \frac{\pi}{2} \right), \tag{4.3}$$

where $a = \eta/(1+\eta^2)$, $g(y) = y^{-1} + 2y$, $h(y) = 3\zeta\big(y + y^3/3\big)/2$,

$$\zeta = \frac{4\pi}{3} \frac{R}{\lambda\gamma^3\sqrt{1+\eta^2}}, \tag{4.4}$$

$$\eta = \frac{eBR}{\gamma m_e} \frac{v_\perp}{v_\parallel^2} \simeq \frac{\omega_c R}{c} \tan\theta, \tag{4.5}$$

R is the tokamak major radius, $J_\nu(x)$ is the Bessel function, $J_\nu'(x)$ its derivative with respect to the argument, and θ is the pitch angle. The parameter η

is the ratio between the perpendicular and drift velocities of the particle and determines how much the radius of curvature (and thus the synchrotron emission) varies along the particle orbit [112, 113]. The parameter ζ is proportional to the ratio $\lambda_{\max}/\lambda$, where $\lambda_{\max}$ is the wavelength where the spectrum peaks (the exact expression for which depends on the parameter regime [113]). The integrands in Eq. (4.3) are products of Bessel functions and trigonometric functions and are highly oscillatory with respect to the variable of integration (y). Because of this, numerical integration – although possible – is not straight-forward. For wavelengths shorter than the maximum, the oscillations become particularly rapid, as ζ (which appears in the arguments of both the Bessel and trigonometric functions) becomes large.

In Ref. [112], two asymptotic forms of Eq. (4.3) are also derived. These use approximations for the integrals, meaning that they are more suited for numerical implementation. In Paper A, the three formulas of Ref. [112], together with Eq. (4.1), are studied and compared for a variety of tokamak parameters and it is concluded that the cylindrical limit (Eq. 4.1) is a good approximation to Eq. (4.3) in large devices, whereas in devices with small major radius, one of the asymptotic expressions is more suitable in terms of approximating Eq. (4.3). In general, however, the power spectra from the various expressions are similar.

4.1.3 Spectrum from a runaway distribution

The total synchrotron power emitted by an electron in circular motion is [104]

$$P_{\mathrm{tot}} = \frac{e^2}{6\pi\varepsilon_0}\,\frac{\omega_\perp}{\rho}\,\beta_\perp^3\gamma^4, \tag{4.6}$$

where $\omega_\perp$ is the angular velocity, ρ is the radius of curvature and $\beta_\perp = v_\perp/c$. In a homogeneous magnetized plasma, the angular velocity and curvature radius are the Larmor frequency and radius, respectively: ω_{c} and $r_{\mathrm{L}} = v_\perp/\omega_{\mathrm{c}}$. This gives

$$P_{\mathrm{tot}} = \frac{e^2}{6\pi\varepsilon_0}\,\frac{\omega_{\mathrm{c}}^2}{v_\perp}\,\beta_\perp^3\gamma^4 = \frac{e^4}{6\pi\varepsilon_0 m_{\mathrm{e}}^2 c}\,B^2\beta_\perp^2\gamma^2 = \frac{e^4}{6\pi\varepsilon_0 m_{\mathrm{e}}^2 c}\,B^2 p_\perp^2. \tag{4.7}$$

The total emitted power thus scales as $p_\perp^2 = \gamma^2(v_\perp/c)^2 = \gamma^2\sin^2\theta\,(v/c)^2 \approx \gamma^2\theta^2$, with θ the particle pitch angle, meaning that the most energetic particles with the largest pitch angles emit most strongly. It has therefore been

assumed that the emission from these particles completely dominates the spectrum, and when interpreting synchrotron spectra and emission patterns, the simplification of considering a mono-energetic beam of electrons with a single pitch – referred to here as the "single-particle approximation" – has frequently been employed (see for instance Refs. [109, 114–116]).

Less approximate synchrotron spectra can be calculated by using the average emission from the entire runaway distribution, according to

$$P(\lambda) = \frac{2\pi}{n_\mathrm{r}} \int_{S_\mathrm{r}} f(p_{||}, p_\perp)\, \mathcal{P}\, p_\perp \mathrm{d}p_\perp \mathrm{d}p_{||} = \int_{S_\mathrm{r}} \bar{P}(p_{||}, p_\perp, \lambda)\, \mathrm{d}p_\perp \mathrm{d}p_{||}, \qquad (4.8)$$

where $\mathcal{P} = \mathcal{P}(p_{||}, p_\perp, \lambda)$ is one of the single particle emission formulas (i.e. Eqs. 4.1 and 4.3), S_r is the runaway region in momentum space, and $\bar{P}$ is the integrand – the contribution to the emitted synchrotron power from a given region of momentum space. Spectra calculated from runaway distributions using the above equation are studied in detail in Papers A and B.

The validity of the single-particle approximation can be assessed by examining the contribution to the total synchrotron emission at a given wavelength from different parts of momentum space. This is done in Fig. 4.2. The figure shows a runaway distribution and the corresponding contribution to the emission (the quantity $\bar{P}$) for two different wavelengths[1]. In this case, the spectrum (calculated using Eq. 4.1) peaks at around 15 µm. At short wavelengths (Fig. 4.2b), the emission is localized to the particles of largest energy and pitch angle, as expected from the simple argument above. At somewhat longer wavelengths (Fig. 4.2c), however; particles in a larger part of momentum space contribute (and the emission is much stronger in general). In addition, for this wavelength, the main contribution is not from the particles with the largest pitch-angle, but $\bar{P}$ instead peaks closer to the parallel axis. Both these effects lead to the single-particle approximation becoming a poor estimate in general (at the very least, different particle energies and pitches would have to be used to approximate the distribution at different wavelengths).

This fact is also evident from the comparison of single-particle and runaway-distribution synchrotron spectra, where the spectra generally differ both qualitatively and quantitatively, as shown in Papers A and B. Including the full runaway distribution in the calculation is thus absolutely necessary to obtain

[1] The parameters used were $T = 300\,\mathrm{eV}$, $n = 5 \cdot 10^{19}\,\mathrm{m}^{-3}$, $E = 1\,\mathrm{V/m}$, $Z_\mathrm{eff} = 1$ and $B = 5.3\,\mathrm{T}$, and the distribution was obtained by running CODE for 17000 collision times, including synchrotron-radiation back-reaction, but neglecting avalanche runaway generation.

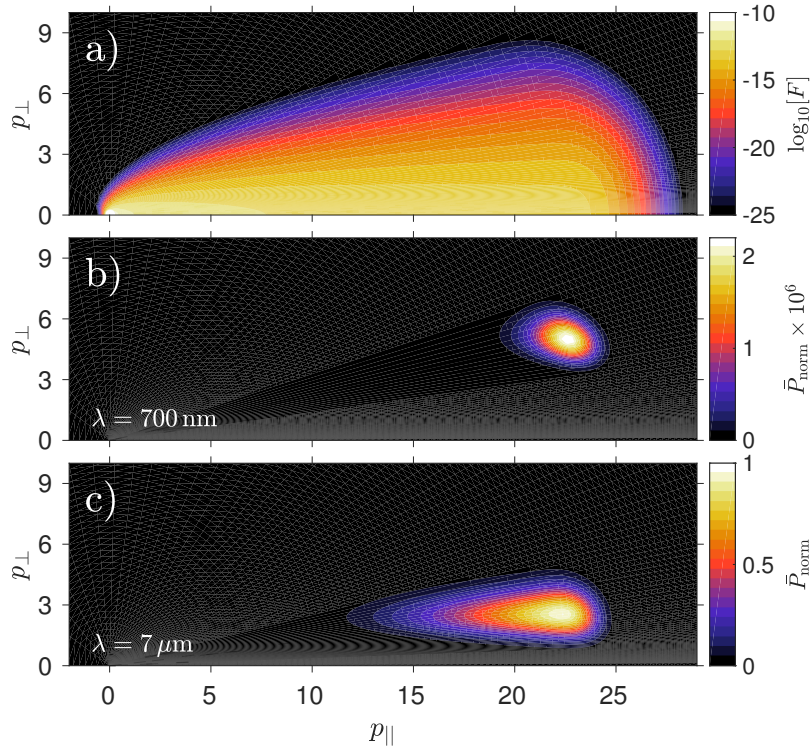

Figure 4.2: a) Electron distribution in 2D momentum space and b)–c) contribution to the corresponding synchrotron emission at wavelengths b) $\lambda = 700\,\mathrm{nm}$ and c) $\lambda = 7\,\mu\mathrm{m}$. The plotted quantity in b) and c) is $\bar{P}_{\mathrm{norm}} = \bar{P}/\max[\bar{P}_{7\mu\mathrm{m}}]$, i.e. $\bar{P}$ normalized to its maximum value for $\lambda = 7\,\mu\mathrm{m}$. Note the difference in emission amplitude for the two wavelengths.

accurate results, and in this sense SYRUP constitutes a significant improvement over previous methods. The synchrotron spectrum is very sensitive to changes in the plasma parameters and electric-field strength. This sensitivity is due to the dependence on the exact shape of the runaway distribution, something which cannot be captured by the mono-energetic approximation.

It is clear from the discussion above that particles of many different energies and pitches contribute to the observed synchrotron spectrum. This is also true for the spatial shape of the detected radiation spot, where particles at different spatial locations and with different momenta contribute to overlapping regions on the detector plane. This added complication makes the task of extracting information about the runaway distribution from the synchrotron image highly non-trivial.

In the analysis in Paper A, analytical avalanche distributions were used. The analytical formula (Eq. 3.7) represents a steady-state limit, however, and is not able to capture dynamical effects or describe the synchrotron emission in the early stages of the runaway-population evolution. In addition, it does not include the effect of radiation-reaction losses, which can have a significant effect when E/E_c is small. In Paper B, numerical distributions from CODE were used to study both dynamic phenomena and distributions where the Dreicer mechanism was dominant. Excellent agreement was also found between the numerical distribution and Eq. (3.7) at sufficiently late times.

4.2 Radiation-reaction force

As an electron emits radiation, it receives an impulse in the opposite direction due to the conservation of momentum. There is therefore a *radiation-reaction force* F_{syn} associated with the emission of synchrotron radiation, which acts to slow the particle down (and reduce its pitch angle). Synchrotron emission only becomes important at relativistic energies, however; contrary to collisional friction, the radiation reaction force increases with particle speed (in accordance with the estimate in the previous section). This completely changes the force balance for runaways at high momentum and non-vanishing pitch angles[2]. In the following discussion it is convenient to consider only the one-dimensional single-particle force balance to qualitatively illustrate the impact of the synchrotron radiation reaction on the dynamics. In practice, however;

[2]The force balance exactly on the parallel axis remains unchanged, as non-vanishing $p_\perp$ is required for the emission of synchrotron radiation.

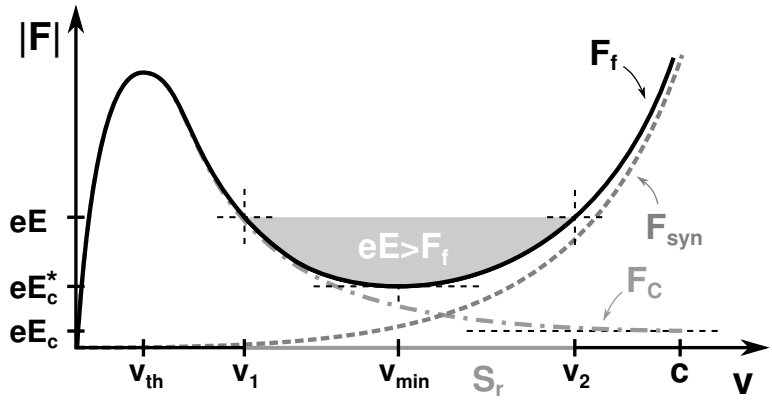

Figure 4.3: Schematic representation of the forces associated with total friction (F_f), collisional friction (F_C), synchrotron radiation reaction (F_syn), the (classical) critical field (E_c) and the critical field including synchrotron radiation reaction (E_c^*). The two critical velocities v_1 and v_2 corresponding to the electric field E are also shown, together with the runaway region (S_r), and the speed at which the total friction force is minimized (v_min). See Fig. 2.2 for comparison. Note that the velocity scale is chosen for clarity – in practice both v_min and v_2 lie close to c.

the problem involves transport processes in two-dimensional momentum space and must in general be treated using numerical tools, see Chapter 3.

The force balance in the presence of synchrotron radiation reaction is depicted in Fig. 4.3. Two effects are of particular interest in the figure: firstly, the radiation-reaction force effectively prevents runaways from reaching arbitrary energies, and secondly, it raises the critical field for runaway generation. We will discuss these two effects in turn in the following sections.

4.2.1 A limit on the achievable runaway energy

As can be seen in Fig. 4.3; for a given electric field E, there are two speeds (v_1 and v_2) larger than the thermal speed for which the total friction force equals the accelerating force: $F_\mathrm{f}(v_{1,2}) = |eE|$. Runaway is only possible for $v_1 < v < v_2$, meaning that particles are unlikely to reach energies significantly higher than that corresponding to v_2. This has been suggested as a possi-

ble mechanism limiting the achievable runaway energy, both in the case of synchrotron and bremsstrahlung radiation reaction [60, 66, 117, 118].

An additional consequence of the existence of an upper bound to the runaway region is that particles tend to accumulate in the vicinity of the speed v_2 in velocity space. Provided certain conditions are satisfied, momentum-space transport mechanisms associated with this process can even lead to the formation of a non-monotonic feature – a "bump" – on the runaway tail, as discussed in Papers G, H and I (not included in the thesis).

4.2.2 Effect on the critical field

As indicated by Fig. 4.3, the minimum of the friction force for any non-vanishing ξ is no longer found at $v = c$ (see Sec. 2.1.1), but at some intermediate speed $v_{\min}$ satisfying $v_1 < v_{\min} < v_2$. (Note that, since the synchrotron emission is a relativistic effect, $v_{\min}$ will nevertheless be close to c.) Therefore, the minimum field necessary for runaway generation to occur is raised accordingly:

$$|eE_{\mathrm{c}}^*(\xi)| = F_{\mathrm{f}}(v_{\min}, \xi), \tag{4.9}$$

where $E_{\mathrm{c}}^*(\xi)$ is the critical field at a given ξ in the presence of radiation reaction forces and $E_{\mathrm{c}}^* > E_{\mathrm{c}}$ for all non-vanishing ξ, as depicted in Fig. 4.3.

Note that the force balance on the parallel axis ($\xi = 1$) remains unaffected by the radiation reaction, and thus the critical field E_{c} is unchanged if collisional diffusion is neglected. In practice, however; diffusive and dynamic processes play an important role in determining the effective critical field. The full problem is studied in Paper D using simulations in `CODE`, and it is found that the synchrotron radiation reaction can reduce the Dreicer growth rate by orders of magnitude for E/E_{c} close to unity, corresponding to an increase in the effective critical field.

4.2.3 Operator for synchrotron radiation reaction

To understand the full role of radiation-reaction effects on plasma dynamics, the single-particle treatment considered above is insufficient. Fully kinetic simulations are necessary to capture the interplay between the various processes affecting the momentum-space transport. Such calculations can be

performed using CODE or NORSE, and for this purpose an operator describing the radiation reaction is needed.

The radiation-reaction force can be calculated from the Abraham-Lorentz-Dirac force affecting an electron [119],

$$\mathbf{F}_{\mathrm{rad}} = \frac{e^2\gamma^2}{6\pi\varepsilon_0 c^3}\left[\ddot{\mathbf{v}} + \frac{3\gamma^2}{c^2}\left(\mathbf{v}\cdot\dot{\mathbf{v}}\right)\dot{\mathbf{v}} + \frac{\gamma^2}{c^2}\left(\mathbf{v}\cdot\ddot{\mathbf{v}} + \frac{3\gamma^2}{c^2}\left(\mathbf{v}\cdot\dot{\mathbf{v}}\right)^2\right)\mathbf{v}\right], \quad (4.10)$$

where $\mathbf{v}$ is the velocity of the particle. Assuming that the magnetic force dominates, so that the particle is predominantly accelerated perpendicular to its velocity ($\mathbf{v}\cdot\dot{\mathbf{v}} = 0$), the expression can be simplified to

$$F^p_{\mathrm{syn}} = -\frac{\gamma p\left(1-\xi^2\right)}{\tau_{\mathrm{r}}} \quad (4.11)$$

$$F^\xi_{\mathrm{syn}} = -\frac{p\xi\sqrt{1-\xi^2}}{\gamma\tau_{\mathrm{r}}}, \quad (4.12)$$

where $\tau_{\mathrm{r}} = 6\pi\varepsilon_0(m_{\mathrm{e}}c)^3/e^4B^2$ is the radiation-damping timescale. The radiation-reaction force enters the kinetic equation (3.2) as an operator of the form $(\partial/\partial\mathbf{p})\cdot(\mathbf{F}_{\mathrm{syn}}f)$, and using Eqs. (4.11) and (4.12), the explicit form is

$$\frac{\partial}{\partial\mathbf{p}}\cdot\left(\mathbf{F}_{\mathrm{syn}}f\right) = -\frac{1-\xi^2}{\gamma\tau_{\mathrm{r}}}\left(\gamma^2 p\frac{\partial f}{\partial p} - \xi\frac{\partial f}{\partial\xi} + \left[4p^2 + \frac{2}{1-\xi^2}\right]f\right). \quad (4.13)$$

The force acts to limit both the particle energy and pitch, which is to be expected as the emitted synchrotron power is proportional to $P_{\mathrm{tot}} \sim \gamma^2\theta^2$ (see Sec. 4.1.3). Fig. 4.4 shows the effect on the distribution: its width in $p_\perp$ and extension in $p_\parallel$ is reduced in the presence of a magnetic field. Equations (4.11) and (4.12) were derived in Ref. [117], the first paper to properly consider the role of radiation reaction in runaway dynamics, but in that paper a high-energy limit was used which lead to an incomplete expression in place of Eq. (4.13), as pointed out in [120].

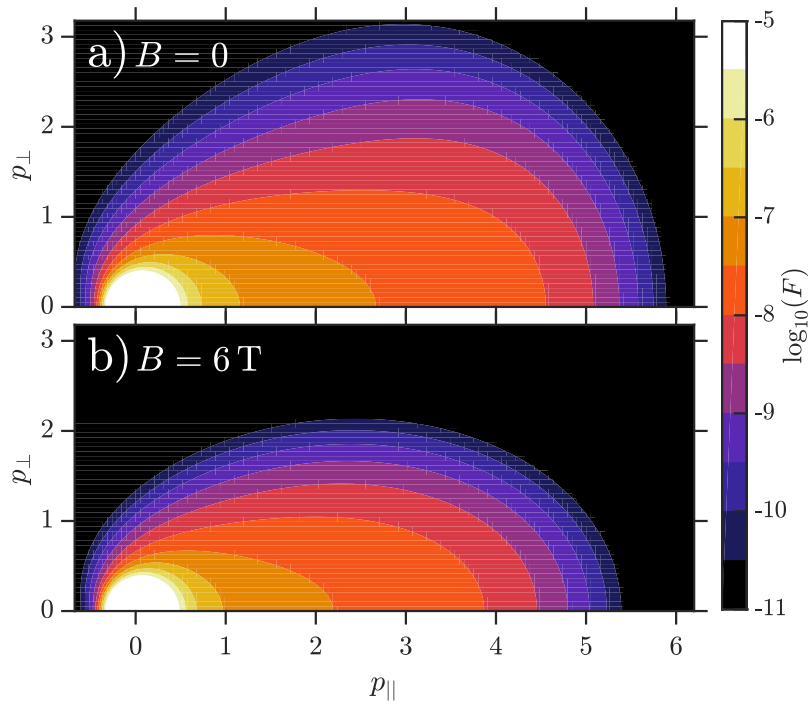

Figure 4.4: Electron distribution functions in CODE after 700 thermal collision times, a) without and b) with synchrotron radiation reaction included. The parameters were $T = 3\,\mathrm{keV}$, $n = 1 \cdot 10^{19}\,\mathrm{m}^{-3}$, $E = 0.05\,\mathrm{V/m}$, $Z_{\mathrm{eff}} = 1$ and $B = 6\,\mathrm{T}$.

5 Nonlinear effects and slide-away

When studying the behavior of runaway electrons, a very common approximation is to treat the runaways as a perturbation to an electron population in local thermal equilibrium. This linearization of the distribution function f around a Maxwellian significantly simplifies the collision operator C_{ee} in Eq. (3.2), as well as the numerical method needed to solve the kinetic equation. However, this approach is not valid when the runaway population becomes substantial, or the linearization becomes invalid for other reasons (such as when a strong electric field $E \gtrsim E_{\mathrm{sa}}$ shifts the bulk of the electron population). There is also a risk that the linearized treatment fails to accurately describe subtle phenomena such as feedback loops (which may for instance cause rapid depletion of the thermal population). The tool `NORSE` was developed to be able to treat such situations, as discussed in Chapter 3. Here we will introduce two particular nonlinear effects considered in Papers E and F: Ohmic heating and slide-away.

5.1 Ohmic heating

The accelerating force of the parallel electric field affects all electrons, not only runaways. However, for most particles, the energy gained from the electric field is quickly redistributed into random motion through collisions with other plasma particles. As a consequence, the electric field acts as a source of heat, primarily affecting the thermal bulk of the electron population – this is commonly referred to as *Ohmic* or *Joule* heating. The associated change in the energy W of the electron population is given by the energy moment of the electric-field term in the kinetic equation:

$$\frac{\mathrm{d}W}{\mathrm{d}\tau} = \int \mathrm{d}^3p\,(\gamma-1)m_{\mathrm{e}}c^2\left(-\frac{\mathbf{E}}{E_{\mathrm{c}}}\cdot\frac{\partial f}{\partial \mathbf{p}}\right), \tag{5.1}$$

with $\tau = \nu_{\mathrm{rel}}t$ the time in units of the collision time for relativistic electrons. If the electric field is sufficiently strong, the heating of the bulk can be sub-

stantial. This can have consequences for electron slide-away, as discussed in the next section.

The Ohmic heating is automatically accounted for in a nonlinear treatment of the kinetic equation, making NORSE able to consistently model this process. This is less straight-forward to do in a linearized tool such as CODE, since the heating effectively involves a change to the Maxwellian around which the distribution is linearized; either the heat must be removed, or the properties of the Maxwellian modified.

The heat supplied by the electric field does not always stay in the plasma, however. Spatial temperature gradients lead to heat transport (a fundamental problem in fusion reactors), although this process may or may not be relevant on the runaway acceleration timescale. More important in a cold post-disruption fusion plasma may be the energy radiated away via atomic transitions in partially ionized impurity ions (the so-called *line radiation*), or spatial transport of particles and energy due to unstable modes (sometimes driven by the runaways themselves – see for instance [90] and Paper K). As a consequence, the plasma temperature may stay constant, or even decrease, despite the existence of a strong electric field.

5.2 Electron slide-away

As discussed in Sec. 2.1.2: if the electric field is stronger than the collisional friction in the entire momentum space, all electrons are accelerated, which is known as the slide-away regime [1, 57]. Recalling that the slide-away field $E_{\mathrm{sa}} \sim n/T$ (see Eq. 2.5), where these quantities are those of the bulk (since the maximum of the friction force is located at around $v = v_{\mathrm{th}}$), a transition to the slide-away regime can be induced through either of the following four mechanisms:

I: $E > E_{\mathrm{sa}}$ – For electric fields stronger than the classical slide-away field E_{sa}, slide-away is immediate

II: $E \lesssim E_{\mathrm{sa}}$ – Although the field is slightly weaker than E_{sa}, it distorts the distribution, which lowers the friction. This process is a positive feedback loop, since the reduced friction makes acceleration easier, leading to further distortion of the distribution, reduced friction, etc. Eventually, the friction is sufficiently reduced that the electric-field acceleration dominates everywhere, leading to slide-away. This process happens on

timescales comparable to the thermal collision time, and is thus very quick.

III: $E < E_{\mathrm{sa}}$, no or inadequate heat sink – The field is significantly weaker than E_{sa} but supplies heat to the distribution. This heat is not efficiently removed, which leads to Ohmic heating of the bulk electrons. The increase in temperature reduces the slide-away field, eventually leading to slide-away as the electric field becomes comparable to $E_{\mathrm{sa}}(t)$. The process can be slow or quick, depending on the initial value of E/E_{sa} and the efficacy of the heat sink.

IV: $E < E_{\mathrm{sa}}$, adequate heat sink – The heat supplied by the electric field is removed and the temperature is kept constant. The electric field causes prolonged substantial runaway generation, which eventually leads to depletion of the bulk population of electrons. This reduces the slide-away field, and eventually slide-away is reached. This process is generally the slowest.

Mechanisms I–III are discussed in Paper E. In Paper F, the focus is the influence on the transition to slide-away of the properties of the heat sink. Both mechanisms III and IV are observed in a tokamak-relevant scenario, depending on the details of the heat sink. The feedback loop related to mechanism II is also discussed, as mechanisms III and IV exhibit the behavior of mechanism II just before slide-away is reached.

In an idealized situation, slide-away should eventually occur in *all* systems with a persistent electric field. In practice, however; this is not observed. If $E \ll E_{\mathrm{sa}}$, the timescale of the slide-away transition is slow compared to most processes in the plasma. In this case, cold electrons are supplied to the thermal population, compensating for the particles running away and thus preventing a transition in accordance with mechanism IV. Also in the absence of efficient cooling (mechanism III), slide-away may be prevented by the feedback between the current and the electric field. The electric field in a tokamak disruption is generated as a consequence of a reduction in the plasma current (due to a quick cooling of the plasma), however if runaway generation becomes strong enough to significantly affect the total current, the electric field will be reduced. This may interrupt a transition through mechanisms III or IV before slide-away is reached. Fields sufficiently strong to cause slide-away through mechanisms I–II are uncommon in fusion experiments. Nevertheless, as demonstrated in Paper F, non-linear simulations can be vital for the understanding of some realistic tokamak scenarios where a linearized approach quickly becomes invalid.

6 Concluding remarks

In order to reduce the threat posed by runaway electrons to future fusion-energy devices, progress on several fronts are necessary. The understanding of runaway generation and loss mechanisms needs to be improved – both theoretically and experimentally – so that reliable operation scenarios and efficient mitigation schemes can be developed. At the core of the runaway phenomenon lies dynamics in momentum space, which is the topic of this thesis. The most important mechanisms affecting these dynamics are summarized schematically in Fig. 6.1. In this thesis, these mechanisms (apart from bremsstrahlung radiation reaction) have been investigated using purpose-built numerical tools, leading to several new insights concerning runaway dynamics. The present Chapter provides a summary of the papers that constitute this work, as well as a short outlook.

6.1 Summary of the included papers

An important component in increasing the understanding of runaway dynamics is to improve the capability to analyze experimentally observed runaway beams and to extract the information available in the few diagnostic measurements that are sensitive to the runaway parameters. To this end, Paper A is focused on calculating the synchrotron spectrum emitted by a distribution of runaway electrons: a significant improvement over previous methods which typically interpret the observed spectra using a single-particle approximation for the runaway population (as discussed in connection with Fig. 4.2). As shown in the paper, this approximation fails to capture both qualitative and quantitative features of the synchrotron spectrum, and the use of distribution-integrated spectra is essential to accurately infer the runaway parameters. The paper analyses the spectra obtained using analytical avalanche distributions (Eq. 3.7). Together with the possibility to easily obtain runaway-electron distribution functions numerically using `CODE` or `NORSE`, the work in this thesis makes a significant contribution to the interpretation of synchrotron spectra, and thereby to the experimental analysis of runaway-electron parameters.

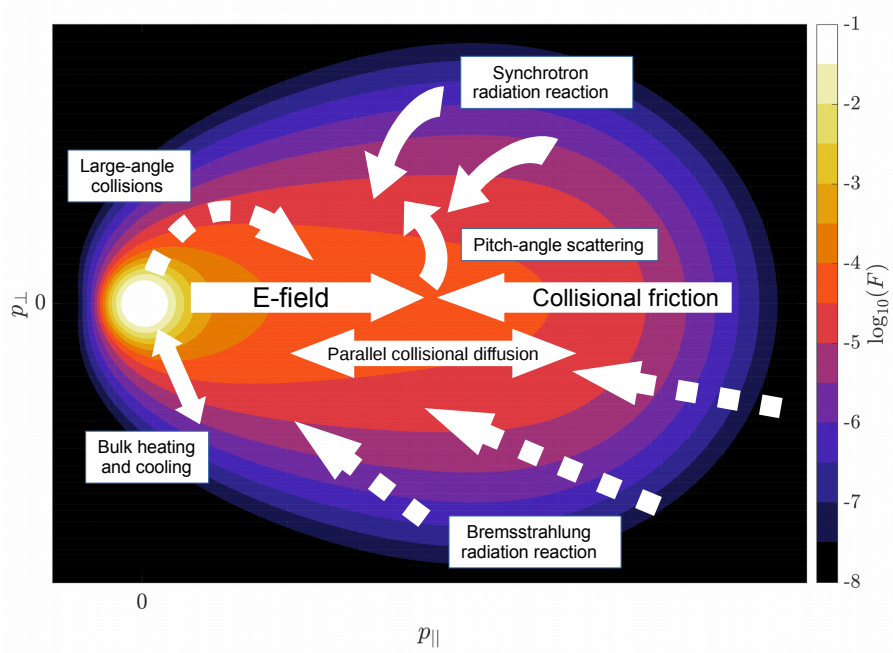

Figure 6.1: Schematic presentation of the various effects of importance for runaway-electron momentum-space dynamics and their qualitative effect on the distribution function. Bremsstrahlung radiation reaction is included for completeness, even though it has not been discussed in detail in this thesis.

Paper B describes and validates the development of CODE, a tool for calculating the time-evolution of the electron distribution function (or its steady-state shape) in the presence of electric-field acceleration and Coulomb collisions. In the paper, the obtained distributions are used to calculate synchrotron spectra (in accordance with Paper A), giving access to parameter regimes and evolution times not properly modeled by the analytical avalanche distribution.

Paper C expands the capability of CODE by introducing time-dependent plasma parameters (enabling the modeling of dynamic scenarios such as disruptions); a conservative collision operator essential for calculating e.g. the plasma conductivity; and the avalanche source term in Eq. (3.5). A scenario dominated by hot-tail runaway generation is investigated, and the effect on the avalanche

growth rate of the choice of avalanche operator is quantified. It is found that the commonly used Rosenbluth-Putvinski avalanche operator can both overestimate and underestimate the avalanche growth rate significantly, depending on the parameter range.

Apart from acting as an observable diagnostic for the runaway distribution, the emission of synchrotron radiation also affects the distribution itself, as discussed in Sec. 4.2. To model this behavior, Paper D introduces an operator describing synchrotron radiation reaction into `CODE` and uses it to investigate the effect of the radiation reaction on the critical field for runaway generation. The paper also explains that a large part of the observed modification to the critical field (initially attributed to so-called "anomalous losses", which include synchrotron radiation reaction) is in fact likely to be just a manifestation of the temperature dependence of the Dreicer runaway-generation rate (Eq. 2.10), so that the parameter determining the runaway growth is E/E_D rather than E/E_c. The paper also shows that redistribution of particles in velocity space can give the impression (because of reduced synchrotron emission) that the runaway population is decaying, when in fact both the number and total kinetic energy of the runaways keep increasing. Again, these insights impact the interpretation of experimental observations and thus contribute to the understanding of runaway parameters in practice.

Paper E describes the development of `NORSE`. The motivation behind this new Fokker-Planck tool was to investigate the impact of collisional nonlinearities on the runaway dynamics. Specifically, `NORSE` makes it possible to study situations where the runaways constitute a substantial part of the electron distribution, or the electric field is significant compared to E_D. This had not previously been done in a framework allowing for relativistic particle energies. The paper highlights the fact that a transition to the slide-away regime can be initiated for electric fields well below the traditional slide-away field E_sa. This line of investigation is then continued in Paper F, which uses an ITER-disruption scenario to explore the importance of Ohmic heating of the bulk electron population. In addition, the paper studies the impact on the slide-away dynamics of the efficiency of the available heat-loss mechanisms. It is found that in the absence of spatial-transport and current–electric-field feedback effects, the electron population in an ITER disruption should eventually transition to a slide-away regime, however the time scale of this transition depends strongly on the heat-loss rate. This could potentially have large consequences for the understanding of runaway dynamics in ITER, although further investigations are needed.

6.2 Outlook

In this thesis, the focus has been on modeling of the dynamics of runaway electrons in momentum space. These dynamics have sometimes been misunderstood or misinterpreted, as in the case of observed modifications to the critical electric field, which motivated the work on Paper D. The tools developed in this thesis can help avoid future such misunderstandings – as they facilitate the investigation of runaway dynamics – and make more accurate interpretation of experimental data possible.

All results presented in this thesis were obtained using predefined electric-field evolutions, i.e. the applied electric field was not affected by the electron distribution in any way and was therefore not calculated self-consistently. As long as the runaway population and current are small, this approximation is adequate, however in cases where the runaways contribute a substantial part of the plasma current (or otherwise significantly affect the plasma evolution), a self-consistent treatment is essential. This point is of particular concern in the scenario considered in Paper F. To build on the work presented here, a logical step forward is to include a self-consistent electric field, taking the evolution of the electron distribution into account.

Another area for further research is to extend the numerical treatment to include one spatial (radial) dimension. This would make it possible to capture magnetic trapping effects, as well as collisional radial transport of the runaways. Naturally, such a development is not without complications, both analytically and numerically, and the increased dimensionality puts much higher demands on the computational resources. Although Fokker-Planck tools (such as `LUKE` [44, 45]) that include a radial coordinate do exist, they are not primarily focused on runaway research. Neither do they necessarily include all the relevant effects (for instance `LUKE` includes trapping effects, but not consistent radial transport).

Some progress towards including the two effects mentioned above have been made, and is described in Conf. Contrib. V. The adopted approach is to couple a Fokker-Planck solver (in this case `CODE`) to the 1D fluid code `GO` [72, 121–123], which evolves the plasma parameters and current, and handles radial electric-field diffusion. This approach could serve as a first step towards a self-consistent model, however further work is needed since `CODE` does not include trapping effects. A complete tool able to consistently calculate the electron distribution function as a function of momentum, radius and time in a disruption scenario would contribute significantly to the understanding

of runaway generation and loss, and would be of great value to the fusion community.

The work presented in this thesis has brought new insights into the dynamics of runaways and the analysis of the radiation they emit. Hopefully, the information and tools described herein will bring us one step closer to stable and reliable operation of fusion devices.

Bibliography

[1] H. Dreicer, Electron and ion runaway in a fully ionized gas I, Physical Review **115**, 238 (1959), DOI: 10.1103/PhysRev.115.238.

[2] H. Dreicer, Electron and ion runaway in a fully ionized gas II, Physical Review **117**, 329 (1960), DOI: 10.1103/PhysRev.117.329.

[3] A. Einstein, Zur Elektrodynamik bewegter Körper, Annalen der Physik **322**, 891 (1905), DOI: 10.1002/andp.19053221004.

[4] P. Helander, L.-G. Eriksson, and F. Andersson, Runaway acceleration during magnetic reconnection in tokamaks, Plasma Physics and Controlled Fusion **44**, B247 (2002), DOI: 10.1088/0741-3335/44/12B/318.

[5] W. J. Nuttall, Fusion as an energy source: Challenges and opportunities, Tech. Rep. (Institute of Physics Report, 2008) http://www.iop.org/publications/iop/2008/file_38224.pdf.

[6] F. F. Chen, *An Indispensable Truth - How Fusion Power Can Save the Planet* (Springer, 2011).

[7] J. P. Freidberg, *Plasma Physics And Fusion Energy* (Cambridge University Press, 2007).

[8] T. Hender, J. Wesley, J. Bialek, A. Bondeson, A. Boozer, R. Buttery, A. Garofalo, T. Goodman, R. Granetz, Y. Gribov, O. Gruber, M. Gryaznevich, G. Giruzzi, S. Günter, N. Hayashi, P. Helander, C. Hegna, D. Howell, D. Humphreys, G. Huysmans, A. Hyatt, A. Isayama, S. Jardin, Y. Kawano, A. Kellman, C. Kessel, H. Koslowski, R. L. Haye, E. Lazzaro, Y. Liu, V. Lukash, J. Manickam, S. Medvedev, V. Mertens, S. Mirnov, Y. Nakamura, G. Navratil, M. Okabayashi, T. Ozeki, R. Paccagnella, G. Pautasso, F. Porcelli, V. Pustovitov, V. Riccardo, M. Sato, O. Sauter, M. Schaffer, M. Shimada, P. Sonato, E. Strait, M. Sugihara, M. Takechi, A. Turnbull, E. Westerhof, D. Whyte, R. Yoshino, H. Zohm, and the ITPA MHD, Disruption

and Magnetic Control Topical Group, Chapter 3: MHD stability, operational limits and disruptions, Nuclear Fusion **47**, S128 (2007), DOI: 10.1088/0029-5515/47/6/S03.

[9] E. Hollmann, G. Arnoux, N. Commaux, N. Eidietis, T. Evans, R. Granetz, A. Huber, D. Humphreys, V. Izzo, A. James, T. Jernigan, M. Lehnen, G. Maddaluno, R. Paccagnella, P. Parks, V. Philipps, M. Reinke, D. Rudakov, F. Saint-Laurent, V. Sizyuk, E. Strait, J. Wesley, C. Wong, and J. Yu, Plasma-surface interactions during tokamak disruptions and rapid shutdowns, Journal of Nuclear Materials **415**, S27 (2011), DOI: 10.1016/j.jnucmat.2010.10.009, Proceedings of the 19th International Conference on Plasma-Surface Interactions in Controlled Fusion.

[10] A. H. Boozer, Theory of runaway electrons in ITER: Equations, important parameters, and implications for mitigation, Physics of Plasmas **22**, 032504 (2015), DOI: 10.1063/1.4913582.

[11] A. Gurevich, G. Milikh, and R. Roussel-Dupre, Nonuniform runaway air-breakdown, Physics Letters A **187**, 197 (1994), DOI: 10.1016/0375-9601(94)90062-0.

[12] H. E. Tierney, R. A. Roussel-Dupré, E. M. D. Symbalisty, and W. H. Beasley, Radio frequency emissions from a runaway electron avalanche model compared with intense, transient signals from thunderstorms, Journal of Geophysical Research **110** (2005), DOI: 10.1029/2004JD005381.

[13] U. S. Inan and N. G. Lehtinen, Production of terrestrial gamma-ray flashes by an electromagnetic pulse from a lightning return stroke, Geophysical Research Letters **32** (2005), DOI: 10.1029/2005GL023702.

[14] T. F. Bell, V. P. Pasko, and U. S. Inan, Runaway electrons as a source of red sprites in the mesosphere, Geophysical Research Letters **22**, 2127 (1995), DOI: 10.1029/95GL02239.

[15] G. D. Holman, Acceleration of runaway electrons and Joule heating in solar flares, Astrophysical Journal **293**, 584 (1985), DOI: 10.1086/163263.

[16] H. Lesch and W. Reich, The origin of monoenergetic electrons in the arc of the galactic center – particle acceleration by magnetic reconnection, Astronomy and Astrophysics **264**, 493 (1992).

[17] T. Fülöp and G. Papp, Runaway positrons in fusion plasmas, Physical Review Letters **108**, 225003 (2012), DOI: 10.1103/PhysRevLett.108.225003.

[18] T. Fülöp and M. Landreman, Ion runaway in lightning discharges, Physical Review Letters **111**, 015006 (2013), DOI: 10.1103/PhysRevLett.111.015006.

[19] T. Fülöp and S. Newton, Alfvénic instabilities driven by runaways in fusion plasmas, Physics of Plasmas **21**, 080702 (2014), DOI: 10.1063/1.4894098.

[20] J. Wesson, *Tokamaks*, 2nd ed. (Oxford Science Publications, 1997).

[21] O. Heaviside, On the electromagnetic effects due to the motion of electrification through a dielectric, Philosophical Magazine **27**, 324 (1889), DOI: 10.1080/14786448908628362.

[22] H. A. Lorentz, *La Théorie electromagnétique de Maxwell et son application aux corps mouvants*, Archives néerlandaises des sciences exactes et naturelles, Vol. 25 (E. J. Brill, 1892) pp. 363–552.

[23] B. Esposito, J. R. Martín-Solís, F. M. Poli, J. A. Mier, R. Sánchez, and L. Panaccione, Dynamics of high energy runaway electrons in the Frascati Tokamak Upgrade, Physics of Plasmas **10**, 2350 (2003), DOI: 10.1063/1.1574328.

[24] H. W. Lu, X. J. Zha, F. C. Zhong, L. Q. Hu, R. J. Zhou, and EAST Team, Investigation of runaway electrons in the current ramp-up by a fully non-inductive lower hybrid current drive on the EAST tokamak, Physica Scripta **87**, 055504 (2013), DOI: 10.1088/0031-8949/87/05/055504.

[25] M. Cheon, J. Kim, Y. An, D. Seo, and H. Kim, Observation of the loss of pre-disruptive runaway electrons in KSTAR ohmic plasma disruptions, Nuclear Fusion **56**, 126004 (2016), DOI: 10.1088/0029-5515/56/12/126004.

[26] J. Wesson, R. Gill, M. Hugon, F. Schüller, J. Snipes, D. Ward, D. Bartlett, D. Campbell, P. Duperrex, A. Edwards, R. Granetz, N. Gottardi, T. Hender, E. Lazzaro, P. Lomas, N. L. Cardozo, K. Mast, M. Nave, N. Salmon, P. Smeulders, P. Thomas, B. Tubbing, M. Turner, and A. Weller, Disruptions in JET, Nuclear Fusion **29**, 641 (1989), DOI: 10.1088/0029-5515/29/4/009.

[27] P. de Vries, M. Johnson, B. Alper, P. Buratti, T. Hender, H. Koslowski, V. Riccardo, and JET-EFDA Contributors, Survey of disruption causes at JET, Nuclear Fusion **51**, 053018 (2011), DOI: 10.1088/0029-5515/51/5/053018.

[28] E. Lenz, Ueber die Bestimmung der Richtung der durch elektrodynamische Vertheilung erregten galvanischen Ströme, Annalen der Physik **107**, 483 (1834), DOI: 10.1002/andp.18341073103.

[29] R. Gill, B. Alper, A. Edwards, L. Ingesson, M. Johnson, and D. Ward, Direct observations of runaway electrons during disruptions in the JET tokamak, Nuclear Fusion **40**, 163 (2000), DOI: 10.1088/0029-5515/40/2/302.

[30] V. Plyusnin, V. Riccardo, R. Jaspers, B. Alper, V. Kiptily, J. Mlynar, S. Popovichev, E. de La Luna, F. Andersson, and JET EFDA contributors, Study of runaway electron generation during major disruptions in JET, Nuclear Fusion **46**, 277 (2006), DOI: 10.1088/0029-5515/46/2/011.

[31] C. Reux, V. Plyusnin, B. Alper, D. Alves, B. Bazylev, E. Belonohy, A. Boboc, S. Brezinsek, I. Coffey, J. Decker, P. Drewelow, S. Devaux, P. de Vries, A. Fil, S. Gerasimov, L. Giacomelli, S. Jachmich, E. Khilkevitch, V. Kiptily, R. Koslowski, U. Kruezi, M. Lehnen, I. Lupelli, P. Lomas, A. Manzanares, A. M. D. Aguilera, G. Matthews, J. Mlynář, E. Nardon, E. Nilsson, C. P. von Thun, V. Riccardo, F. Saint-Laurent, A. Shevelev, G. Sips, C. Sozzi, and JET contributors, Runaway electron beam generation and mitigation during disruptions at JET-ILW, Nuclear Fusion **55**, 093013 (2015), DOI: 10.1088/0029-5515/55/9/093013.

[32] E. Hollmann, P. Parks, D. Humphreys, N. Brooks, N. Commaux, N. Eidietis, T. Evans, R. Isler, A. James, T. Jernigan, J. Munoz, E. Strait, C. Tsui, J. Wesley, and J. Yu, Effect of applied toroidal electric field on the growth/decay of plateau-phase runaway electron currents in DIII-D, Nuclear Fusion **51**, 103026 (2011), DOI: 10.1088/0029-5515/51/10/103026.

[33] E. Hollmann, M. Austin, J. Boedo, N. Brooks, N. Commaux, N. Eidietis, D. Humphreys, V. Izzo, A. James, T. Jernigan, A. Loarte, J. Martin-Solis, R. Moyer, J. Muñoz-Burgos, P. Parks, D. Rudakov, E. Strait, C. Tsui, M. V. Zeeland, J. Wesley, and J. Yu, Control and dissipation of runaway electron beams created during rapid shutdown experiments in DIII-D, Nuclear Fusion **53**, 083004 (2013), DOI: 10.1088/0029-5515/53/8/083004.

[34] E. Marmar, A. Bader, M. Bakhtiari, H. Barnard, W. Beck, I. Bespamyatnov, A. Binus, P. Bonoli, B. Bose, M. Bitter, I. Cziegler, G. Dekow, A. Dominguez, B. Duval, E. Edlund, D. Ernst, M. Ferrara, C. Fiore, T. Fredian, A. Graf, R. Granetz, M. Greenwald, O. Grulke, D. Gwinn, S. Harrison, R. Harvey, T. Hender, J. Hosea, K. Hill, N. Howard, D. Howell, A. Hubbard, J. Hughes, I. Hutchinson, A. Ince-Cushman, J. Irby, V. Izzo, A. Kanojia, C. Kessel, J. Ko, P. Koert, B. LaBombard, C. Lau, L. Lin, Y. Lin, B. Lipschultz, J. Liptac, Y. Ma, K. Marr, M. May, R. McDermott, O. Meneghini, D. Mikkelsen, R. Ochoukov, R. Parker, C. Phillips, P. Phillips, Y. Podpaly, M. Porkolab, M. Reinke, J. Rice, W. Rowan, S. Scott, A. Schmidt, J. Sears, S. Shiraiwa, A. Sips, N. Smick, J. Snipes, J. Stillerman, Y. Takase, D. Terry, J. Terry, N. Tsujii, E. Valeo, R. Vieira, G. Wallace, D. Whyte, J. Wilson, S. Wolfe, G. Wright, J. Wright, S. Wukitch, G. Wurden, P. Xu, K. Zhurovich, J. Zaks, and S. Zweben, Overview of the Alcator C-Mod research program, Nuclear Fusion **49**, 104014 (2009), DOI: 10.1088/0029-5515/49/10/104014.

[35] F. Saint-Laurent, G. Martin, T. Alarcon, A. L. Luyer, P. B. Parks, P. Pastor, S. Putvinski, C. Reux, J. Bucalossi, S. Bremond, and P. Moreau, Overview of runaway electron control and mitigation experiments on Tore Supra and lessons learned in view of ITER, Fusion Science and Technology **64**, 711 (2013).

[36] Z. Y. Chen, W. C. Kim, Y. W. Yu, A. C. England, J. W. Yoo, S. H. Hahn, S. W. Yoon, K. D. Lee, Y. K. Oh, J. G. Kwak, and M. Kwon, Study of runaway current generation following disruptions in KSTAR, Plasma Physics and Controlled Fusion **55**, 035007 (2013), DOI: 10.1088/0741-3335/55/3/035007.

[37] M. Vlainic, J. Mlynar, J. Cavalier, V. Weinzettl, R. Paprok, M. Imrisek, O. Ficker, M. Varavin, P. Vondracek, and J.-M. Noterdaeme, Post-disruptive runaway electron beams in the COMPASS tokamak, Journal of Plasma Physics **81**, 475810506 (2015), DOI: 10.1017/S0022377815000914.

[38] G. Pautasso, P. McCarthy, C. Fuchs, R. Dux, S. Potzel, G. Papp, M. Sertoli, G. Tardini, K. Lackner, A. Scarabosio, A.Mlynek, L. Giannone, the ASDEX Upgrade team, and the EUROfusion MST team, Generation and suppression of runaway electrons in ASDEX Upgrade disruptions, Europhysics Conference Abstracts **39E**, P1.134 (2015), http://ocs.ciemat.es/EPS2015PAP/pdf/P1.134.pdf.

[39] G. Papp, G. Pautasso, J. Decker, M. Gobbin, P. McCarthy, P. Blanchard, D. Carnevale, D. Choi, S. Coda, B. Duval, R. Dux, B. Erdős, B. Esposito, O. Ficker, R. Fischer, C. Fuchs, C. Galperti, L. Giannone, A. Gude, B. Labit, K. Lackner, T. Lunt, L. Marelli, P. Martin, A. Mlynek, E. Nardon, M. Maraschek, P. Marmillod, M. Nocente, Y. Peysson, P. Piovesan, V. Plyusnin, G. Pokol, P. Poloskei, S. Potzel, C. Reux, F. Saint-Laurent, O. Sauter, B. Sieglin, U. Sheikh, C. Sommariva, W. Suttrop, G. Tardini, M. Teschke, D. Testa, W. Treutterer, M. Valisa, ASDEX Upgrade Team, TCV Team, and the EUROfusion MST1 Team, Runaway electron generation and mitigation on the european medium sized tokamaks ASDEX Upgrade and TCV, Proceedings of the IAEA Fusion Energy Conference, Kyoto, Japan, EX/9–4 (2016).

[40] C. Barnes and J. Strachan, Sawtooth oscillations in the flux of runaway electrons to the PLT limiter, Nuclear Fusion **22**, 1090 (1982), DOI: 10.1088/0029-5515/22/8/010.

[41] C. Paz-Soldan, N. W. Eidietis, R. Granetz, E. M. Hollmann, R. A. Moyer, J. C. Wesley, J. Zhang, M. E. Austin, N. A. Crocker, A. Wingen, and Y. Zhu, Growth and decay of runaway electrons above the critical electric field under quiescent conditions, Physics of Plasmas **21**, 022514 (2014), DOI: 10.1063/1.4866912.

[42] R. S. Granetz, B. Esposito, J. H. Kim, R. Koslowski, M. Lehnen, J. R. Martin-Solis, C. Paz-Soldan, T. Rhee, J. C. Wesley, L. Zeng, and ITPA MHD Group, An ITPA joint experiment to study runaway electron generation and suppression, Physics of Plasmas **21**, 072506 (2014), DOI: 10.1063/1.4886802.

[43] J. R. Martín-Solís, B. Esposito, R. Sánchez, F. M. Poli, and L. Panaccione, Enhanced production of runaway electrons during a disruptive termination of discharges heated with lower hybrid power in the Frascati Tokamak Upgrade, Physical Review Letters **97**, 165002 (2006), DOI: 10.1103/PhysRevLett.97.165002.

[44] Y. Peysson, J. Decker, and R. W. Harvey, Advanced 3-D electron fokker-planck transport calculations, AIP Conference Proceedings **694**, 495 (2003), DOI: 10.1063/1.1638086.

[45] J. Decker and Y. Peysson, DKE: A fast numerical solver for the 3D drift kinetic equation, Tech. Rep. EUR-CEA-FC-1736 (Euratom-CEA, 2004).

[46] E. Nilsson, J. Decker, Y. Peysson, R. S. Granetz, F. Saint-Laurent, and M. Vlainic, Kinetic modelling of runaway electron avalanches in tokamak

plasmas, Plasma Physics and Controlled Fusion **57**, 095006 (2015), DOI: 10.1088/0741-3335/57/9/095006.

[47] S. Chiu, M. Rosenbluth, R. Harvey, and V. Chan, Fokker-Planck simulations mylb of knock-on electron runaway avalanche and bursts in tokamaks, Nuclear Fusion **38**, 1711 (1998), DOI: 10.1088/0029-5515/38/11/309.

[48] R. W. Harvey, V. S. Chan, S. C. Chiu, T. E. Evans, M. N. Rosenbluth, and D. G. Whyte, Runaway electron production in DIII-D killer pellet experiments, calculated with the CQL3D/KPRAD model, Physics of Plasmas **7**, 4590 (2000), DOI: 10.1063/1.1312816.

[49] E. M. Hollmann, P. B. Aleynikov, T. Fülöp, D. A. Humphreys, V. A. Izzo, M. Lehnen, V. E. Lukash, G. Papp, G. Pautasso, F. Saint-Laurent, and J. A. Snipes, Status of research toward the ITER disruption mitigation system, Physics of Plasmas **22**, 021802 (2015), DOI: 10.1063/1.4901251.

[50] M. Rosenbluth and S. Putvinski, Theory for avalanche of runaway electrons in tokamaks, Nuclear Fusion **37**, 1355 (1997), DOI: 10.1088/0029-5515/37/10/I03.

[51] ITER physics basis, Nuclear Fusion **39**, 2137 (1999).

[52] http://www.iter.org.

[53] M. Lehnen, K. Aleynikova, P. Aleynikov, D. Campbell, P. Drewelow, N. Eidietis, Y. Gasparyan, R. Granetz, Y. Gribov, N. Hartmann, E. Hollmann, V. Izzo, S. Jachmich, S.-H. Kim, M. Kočan, H. Koslowski, D. Kovalenko, U. Kruezi, A. Loarte, S. Maruyama, G. Matthews, P. Parks, G. Pautasso, R. Pitts, C. Reux, V. Riccardo, R. Roccella, J. Snipes, A. Thornton, and P. de Vries, Disruptions in ITER and strategies for their control and mitigation, Journal of Nuclear Materials **463**, 39 (2015), DOI: 10.1016/j.jnucmat.2014.10.075, proceedings of the 21st International Conference on Plasma-Surface Interactions in Controlled Fusion Devices Kanazawa, Japan May 26-30, 2014.

[54] P. Helander and D. J. Sigmar, *Collisional Transport in Magnetized Plasmas* (Cambridge University Press, 2002).

[55] F. F. Chen, *Introduction to plasma physics and controlled fusion*, 2nd ed., Vol. 1 (Plenum Press, 1984).

[56] J. Connor and R. Hastie, Relativistic limitations on runaway electrons, Nuclear Fusion **15**, 415 (1975), DOI: 10.1088/0029-5515/15/3/007.

[57] B. Coppi, F. Pegoraro, R. Pozzoli, and G. Rewoldt, Slide-away distributions and relevant collective modes in high-temperature plasmas, Nuclear Fusion **16**, 309 (1976).

[58] G. Fussmann, On the motion of runaway electrons in momentum space, Nuclear Fusion **19**, 327 (1979), DOI: 10.1088/0029-5515/19/3/005.

[59] H. Smith, P. Helander, L.-G. Eriksson, and T. Fülöp, Runaway electron generation in a cooling plasma, Physics of Plasmas **12**, 122505 (2005), DOI: 10.1063/1.2148966.

[60] J. R. Martín-Solís, J. D. Alvarez, R. Sánchez, and B. Esposito, Momentum-space structure of relativistic runaway electrons, Physics of Plasmas **5**, 2370 (1998), DOI: 10.1063/1.872911.

[61] P. Aleynikov and B. N. Breizman, Theory of two threshold fields for relativistic runaway electrons, Physical Review Letters **114**, 155001 (2015), DOI: 10.1103/PhysRevLett.114.155001.

[62] C. Liu, D. P. Brennan, A. Bhattacharjee, and A. H. Boozer, Adjoint fokker-planck equation and runaway electron dynamics, Physics of Plasmas **23**, 010702 (2016), DOI: 10.1063/1.4938510.

[63] J. R. Martín-Solís, R. Sánchez, and B. Esposito, On the effect of synchrotron radiation and magnetic fluctuations on the avalanche runaway growth rate, Physics of Plasmas **7**, 3814 (2000), DOI: 10.1063/1.1287215.

[64] Y. A. Sokolov, "Multiplication" of accelerated electrons in a tokamak, JETP Letters **29**, 218 (1979).

[65] N. Besedin and I. Pankratov, Stability of a runaway electron beam, Nuclear Fusion **26**, 807 (1986), DOI: 10.1088/0029-5515/26/6/009.

[66] R. Jayakumar, H. Fleischmann, and S. Zweben, Collisional avalanche exponentiation of runaway electrons in electrified plasmas, Physics Letters A **172**, 447 (1993), DOI: 10.1016/0375-9601(93)90237-T.

[67] A. V. Gurevich, On the theory of runaway electrons, Sov. Phys. JETP **12**, 904 (1961).

[68] M. D. Kruskal and I. B. Bernstein, PPPL report MATT-Q-20, p. 174, (1962).

[69] R. H. Cohen, Runaway electrons in an impure plasma, Physics of Fluids **19**, 239 (1976), DOI: 10.1063/1.861451.

[70] S. Putvinski, P. Barabaschi, N. Fujisawa, N. Putvinskaya, M. N. Rosenbluth, and J. Wesley, Halo current, runaway electrons and disruption mitigation in ITER, Plasma Physics and Controlled Fusion **39**, B157 (1997), DOI: http://dx.doi.org/10.1088/0741-3335/39/12B/013.

[71] P. Helander, H. Smith, T. Fülöp, and L.-G. Eriksson, Electron kinetics in a cooling plasma, Physics of Plasmas **11**, 5704 (2004), DOI: 10.1063/1.1812759.

[72] H. Smith, P. Helander, L.-G. Eriksson, D. Anderson, M. Lisak, and F. Andersson, Runaway electrons and the evolution of the plasma current in tokamak disruptions, Physics of Plasmas **13**, 102502 (2006), DOI: 10.1063/1.2358110.

[73] H. M. Smith and E. Verwichte, Hot tail runaway electron generation in tokamak disruptions, Physics of Plasmas **15**, 072502 (2008), DOI: http://dx.doi.org/10.1063/1.2949692.

[74] H. M. Smith, T. Fehér, T. Fülöp, K. Gál, and E. Verwichte, Runaway electron generation in tokamak disruptions, Plasma Physics and Controlled Fusion **51**, 124008 (2009), DOI: 10.1088/0741-3335/51/12/124008.

[75] D. Mosher, Interactions of relativistic electron beams with high atomic-number plasmas, Physics of Fluids **18**, 846 (1975), DOI: 10.1063/1.861219.

[76] Y. L. Igitkhanov, The effect of non-Coulomb scattering of relativistic electrons on the generation of runaways in multicomponent plasma, Contributions to Plasma Physics **52**, 460 (2012), DOI: 10.1002/ctpp.201210034.

[77] K. Aleynikova, P. Aleynikov, S. Konovalov, A. Teplukhina, and V. Zhogolev, Interaction of runaway electrons with high-Z impurities, Europhysics Conference Abstracts **37D**, O5.103 (2013), http://ocs.ciemat.es/EPS2013PAP/pdf/O5.103.pdf.

[78] J. R. Martín-Solís, A. Loarte, and M. Lehnen, Runaway electron dynamics in tokamak plasmas with high impurity content, Physics of Plasmas **22**, 092512 (2015), DOI: 10.1063/1.4931166.

[79] L. Hesslow, *Effect of Screened Nuclei on Fast Electron Beam Dynamics*, Master's thesis, Chalmers University of Technology (2016), http://publications.lib.chalmers.se/records/fulltext/236294/236294.pdf.

[80] G. Papp, M. Drevlak, T. Fülöp, and P. Helander, Runaway electron drift orbits in magnetostatic perturbed fields, Nuclear Fusion **51**, 043004 (2011), DOI: 10.1088/0029-5515/51/4/043004.

[81] G. Papp, M. Drevlak, T. Fülöp, and G. I. Pokol, The effect of resonant magnetic perturbations on runaway electron transport in ITER, Plasma Physics and Controlled Fusion **54**, 125008 (2012), DOI: 10.1088/0741-3335/54/12/125008.

[82] G. Papp, M. Drevlak, G. Pokol, and T. Fülöp, Energetic electron transport in the presence of magnetic perturbations in magnetically confined plasmas, Journal of Plasma Physics **81**, 475810503 (2015), DOI: 10.1017/S0022377815000537.

[83] H. Knoepfel and D. Spong, Runaway electrons in toroidal discharges, Nuclear Fusion **19**, 785 (1979), DOI: 10.1088/0029-5515/19/6/008.

[84] X. Guan, H. Qin, and N. J. Fisch, Phase-space dynamics of runaway electrons in tokamaks, Physics of Plasmas **17**, 092502 (2010), DOI: 10.1063/1.3476268.

[85] L. Zeng, H. R. Koslowski, Y. Liang, A. Lvovskiy, M. Lehnen, D. Nicolai, J. Pearson, M. Rack, H. Jaegers, K. H. Finken, K. Wongrach, Y. Xu, and the TEXTOR team, Experimental observation of a magnetic-turbulence threshold for runaway-electron generation in the TEXTOR tokamak, Physical Review Letters **110**, 235003 (2013), DOI: 10.1103/PhysRevLett.110.235003.

[86] G. Papp, P. W. Lauber, M. Schneller, S. Braun, H. R. Koslowski, and the TEXTOR Team, Interaction of runaway populations with fast particle driven modes, Europhysics Conference Abstracts **38F**, P2.032 (2014), http://ocs.ciemat.es/EPS2014PAP/pdf/P2.032.pdf.

[87] P. Aleynikov and B. Breizman, Stability analysis of runaway-driven waves in a tokamak, Nuclear Fusion **55**, 043014 (2015), DOI: 10.1088/0029-5515/55/4/043014.

[88] Y. Liu, Y. Dong, X. Peng, C. Chen, Y. Zhang, J. Gao, O. Pan, and X. Duan, Mitigation of runaway current with supersonic molecular beam injection on HL-2A tokamak, 26th IAEA Fusion Energy Conference, Kyoto, Japan, EX/9–3 (2016).

[89] T. Fülöp, G. Pokol, P. Helander, and M. Lisak, Destabilization of magnetosonic-whistler waves by a relativistic runaway beam, Physics of Plasmas **13**, 062506 (2006), DOI: 10.1063/1.2208327.

[90] G. Pokol, T. Fülöp, and M. Lisak, Quasi-linear analysis of whistler waves driven by relativistic runaway beams in tokamaks, Plasma Physics and Controlled Fusion **50**, 045003 (2008), DOI: 10.1088/0741-3335/50/4/045003.

[91] A. Kómár, G. I. Pokol, and T. Fülöp, Electromagnetic waves destabilized by runaway electrons in near-critical electric fields, Physics of Plasmas **20**, 012117 (2013), DOI: 10.1063/1.4776666.

[92] A. Kómár, G. I. Pokol, and T. Fülöp, Interaction of electromagnetic waves and suprathermal electrons in the near-critical electric field limit, Journal of Physics: Conference Series **401**, 012012 (2012), DOI: 10.1088/1742-6596/401/1/012012.

[93] L. D. Landau, Kinetic equation for the Coulomb effect, Physikalische Zeitschrift der Sowjetunion **10**, 154 (1936).

[94] M. N. Rosenbluth, W. M. MacDonald, and D. L. Judd, Fokker-Planck equation for an inverse-square force, Physical Review **107**, 1 (1957), DOI: 10.1103/PhysRev.107.1.

[95] S. T. Beliaev and G. I. Budker, The relativistic kinetic equation, Soviet Physics-Doklady **1**, 218 (1956).

[96] B. J. Braams and C. F. F. Karney, Differential form of the collision integral for a relativistic plasma, Physical Review Letters **59**, 1817 (1987), DOI: 10.1103/PhysRevLett.59.1817.

[97] B. J. Braams and C. F. F. Karney, Conductivity of a relativistic plasma, Physics of Fluids B: Plasma Physics **1**, 1355 (1989), DOI: 10.1063/1.858966.

[98] O. Embréus, *Kinetic modelling of runaway in plasmas*, Licentiate thesis, Chalmers University of Technology (2016), http://publications.lib.chalmers.se/records/fulltext/236745/236745.pdf.

[99] C. Møller, Zur theorie des durchgangs schneller elektronen durch materie, Annalen der Physik **406**, 531 (1932), DOI: 10.1002/andp.19324060506.

[100] J. D. Jackson, *Classical Electrodynamics*, 3rd ed. (Wiley & Sons, 1999).

[101] F. R. Elder, A. M. Gurewitsch, R. V. Langmuir, and H. C. Pollock, Radiation from electrons in a synchrotron, Physical Review **71**, 829 (1947), DOI: 10.1103/PhysRev.71.829.5.

[102] E.-E. Koch, *Handbook on Synchrotron Radiation*, Vol. 1a (North Holland, 1983).

[103] G. A. Schott, *Electromagnetic Radiation* (Cambridge University Press, 1912).

[104] J. Schwinger, On the classical radiation of accelerated electrons, Physical Review **75**, 1912 (1949), DOI: 10.1103/PhysRev.75.1912.

[105] G. Bekefi, *Radiation Processes in Plasmas* (Wiley & Sons, 1966).

[106] L. D. Landau and E. M. Lifshitz, *The Classical Theory of Fields*, 4th ed., Course of Theoretical Physics, Vol. 2 (Butterworth-Heinemann, 1975).

[107] K. Finken, J. Watkins, D. Rusbuldt, W. Corbett, K. Dippel, D. Goebel, and R. Moyer,
Observation of infrared synchrotron radiation from tokamak runaway electrons in TEXTOR,
Nuclear Fusion **30**, 859 (1990), DOI: 10.1088/0029-5515/30/5/005.

[108] K. Wongrach, K. Finken, S. Abdullaev, R. Koslowski, O. Willi, L. Zeng, and the TEXTOR Team, Measurement of synchrotron radiation from runaway electrons during the TEXTOR tokamak disruptions, Nuclear Fusion **54**, 043011 (2014), DOI: 10.1088/0029-5515/54/4/043011.

[109] J. H. Yu, E. M. Hollmann, N. Commaux, N. W. Eidietis, D. A. Humphreys, A. N. James, T. C. Jernigan, and R. A. Moyer, Visible imaging and spectroscopy of disruption runaway electrons in DIII-D, Physics of Plasmas **20**, 042113 (2013), DOI: 10.1063/1.4801738.

[110] B. Esposito, L. Boncagni, P. Buratti, D. Carnevale, F. Causa, M. Gospodarczyk, J. Martin-Solis, Z. Popovic, M. Agostini, G. Apruzzese, W. Bin, C. Cianfarani, R. D. Angelis, G. Granucci, A. Grosso, G. Maddaluno, D. Marocco, V. Piergotti, A. Pensa, S. Podda, G. Pucella, G. Ramogida, G. Rocchi, M. Riva, A. Sibio, C. Sozzi, B. Tilia, O. Tudisco, M. Valisa, and FTU Team, Runaway electron generation and control, Plasma Physics and Controlled Fusion **59**, 014044 (2017), DOI: 10.1088/0741-3335/59/1/014044.

[111] R. J. Zhou, L. Q. Hu, E. Z. Li, M. Xu, G. Q. Zhong, L. Q. Xu, S. Y. Lin, J. Z. Zhang, and the EAST Team, Investigation of ring-like runaway electron beams in the EAST tokamak, Plasma Physics and Controlled Fusion **55**, 055006 (2013), DOI: 10.1088/0741-3335/55/5/055006.

[112] I. M. Pankratov, Analysis of the synchrotron radiation spectra of runaway electrons, Plasma Physics Reports **25**, 145 (1999).

[113] I. M. Pankratov, I. V. Pavlenko, and O. A. Pomazan, Analysis of synchrotron radiation emitted by runaway electrons in tokamaks, Journal of Kharkiv National University **1059**, 39 (2013), series "Nuclei, Particles, Fields".

[114] I. M. Pankratov, Analysis of the synchrotron radiation emitted by runaway electrons, Plasma Physics Reports **22**, 535 (1996).

[115] R. Jaspers, N. J. L. Cardozo, A. J. H. Donné, H. L. M. Widdershoven, and K. H. Finken, A synchrotron radiation diagnostic to observe relativistic runaway electrons in a tokamak plasma, Review of Scientific Instruments **72**, 466 (2001), DOI: 10.1063/1.1318245.

[116] R. J. Zhou, I. M. Pankratov, L. Q. Hu, M. Xu, and J. H. Yang, Synchrotron radiation spectra and synchrotron radiation spot shape of runaway electrons in Experimental Advanced Superconducting Tokamak, Physics of Plasmas **21**, 063302 (2014), DOI: 10.1063/1.4881469.

[117] F. Andersson, P. Helander, and L.-G. Eriksson, Damping of relativistic electron beams by synchrotron radiation, Physics of Plasmas **8**, 5221 (2001), DOI: 10.1063/1.1418242.

[118] M. Bakhtiari, G. J. Kramer, M. Takechi, H. Tamai, Y. Miura, Y. Kusama, and Y. Kamada, Role of bremsstrahlung radiation in limiting the energy of runaway electrons in tokamaks, Physical Review Letters **94**, 215003 (2005), DOI: 10.1103/PhysRevLett.94.215003.

[119] W. Pauli, *Theory of Relativity* (Dover, New York, 1981).

[120] R. Hazeltine and S. Mahajan, Radiation reaction in fusion plasmas, Physical Review E **70**, 046407 (2004), DOI: 10.1103/PhysRevE.70.046407.

[121] L.-G. Eriksson, P. Helander, F. Andersson, D. Anderson, and M. Lisak, Current dynamics during disruptions in large tokamaks, Physical Review Letters **92**, 205004 (2004), DOI: 10.1103/PhysRevLett.92.205004.

[122] K. Gál, T. Fehér, H. Smith, T. Fülöp, and P. Helander, Runaway electron generation during plasma shutdown by killer pellet injection, Plasma Physics and Controlled Fusion **50**, 055006 (2008).

[123] T. Fehér, H. M. Smith, T. Fülöp, and K. Gál, Simulation of runaway electron generation during plasma shutdown by impurity injection in ITER, Plasma Physics and Controlled Fusion **53**, 035014 (2011).